

hep-ph/9509316

PM/95-30

THES-TP 95/08

September 1995

Corrected version, November 1995

Tests of Anomalous Higgs Boson Couplings through $e^-e^+ \rightarrow ZH$ and γH ¹

G.J. Gounaris^a, F.M. Renard^b and N.D. Vlachos^a

^aDepartment of Theoretical Physics, University of Thessaloniki,
 Gr-54006, Thessaloniki, Greece,

^bPhysique Mathématique et Théorique, CNRS-URA 768,
 Université de Montpellier II, F-34095 Montpellier Cedex 5.

Abstract

We show how the processes $e^-e^+ \rightarrow ZH$, γH , which will be studied at LEP2 and at high energy colliders, could be used to search for types of New Physics (NP) characterized by an effective NP scale in the few TeV range and affecting the scalar sector only. In particular, for $e^-e^+ \rightarrow ZH$, we propose the measurement of suitable azimuthal asymmetries determined from the angular distribution of the Z -decay plane with respect to the Z -production one. Such asymmetries, together with the ZH angular distribution, may allow a complete disentangling of the five $dim = 6$ operators \mathcal{O}_{UB} , \mathcal{O}_{UW} , $\overline{\mathcal{O}}_{UB}$, $\overline{\mathcal{O}}_{UW}$, $\mathcal{O}_{\Phi 2}$, describing the residual NP effects to the Higgs couplings. We note that the first four of these operators contribute to processes relevant to LEP1 precision measurements only at the 1-loop level, while the last operator remains completely unconstrained at this level. The process $e^-e^+ \rightarrow \gamma H$ is also very sensitive to NP and should bring important independent information.

¹Partially supported by the EC contract CHRX-CT94-0579.

1 Introduction

The scalar sector is the most mysterious part of the Standard Model (SM) of the electroweak interactions and the favorite place for generating New Physics (NP) manifestations [1, 2]. If it happens that all new particles are too heavy to be directly produced at future colliders, then the only way NP could manifest itself, is through residual interactions affecting the particles already present in SM. The possibility for such residual NP effects involving the interactions of the gauge bosons with the leptons and the light quarks [3, 4], has already been essentially excluded by LEP1 [5]. Thus, only in self-interactions among the gauge and Higgs bosons [6] and possibly also the heavy quarks [7], there appears to be still room for some NP.

In the following, we will concentrate on types of NP affecting the purely weak boson sector only. Those involving the gauge bosons only (like *e.g.* the γWW and ZWW couplings) will be constrained by $e^-e^+ \rightarrow W^-W^+$ at LEP2 [8, 9] and NLC [10], as well as by other gauge boson pair production processes [11, 12, 13]. Assuming that this has been done and nothing new has been found, then the only remaining possibility for NP in the purely bosonic sector will be hidden in interactions involving the physical Higgs boson. This assumes of course that the Higgs particle exists and has a mass comparable to M_W . Supposing that the NP scale satisfies $\Lambda_{NP} \gg M_W$ and that it is justified to restrict to $SU(2) \times U(1)$ gauge invariant $dim = 6$ operators only, the NP should then be determined by the four "blind" operators \mathcal{O}_{UB} , \mathcal{O}_{UW} and their CP -violating partners $\overline{\mathcal{O}}_{UB}$, $\overline{\mathcal{O}}_{UW}$, as well as the "superblind" operator $\mathcal{O}_{\Phi 2}$ [4, 6, 14]. This possibility is also motivated by a recent treatment suggesting that it is much easier to create anomalous NP interactions for the Higgs particle than for the gauge bosons [15, 14]. The basic reason for this is that Higgs couplings enjoy the familiar Yukawa type freedom, while the gauge boson interactions are strongly constrained by the gauge principle.

It is important to state that the operators \mathcal{O}_{UB} , \mathcal{O}_{UW} , $\overline{\mathcal{O}}_{UB}$, $\overline{\mathcal{O}}_{UW}$, are only mildly constrained (at the 1-loop level) by LEP1 precision measurements, as opposed to a number of other $dim = 6$ operators which are strongly constrained through their non-vanishing tree level contributions. In a sense, these operators cannot "see" LEP1 and they have thus been called "blind" [3, 4]. In that respect, the operator $\mathcal{O}_{\Phi 2}$ is "superblind", since it is insensitive to LEP1 measurements even at 1-loop. It turns out that at tree level and up to first order in the anomalous couplings, $\mathcal{O}_{\Phi 2}$ is also insensitive to the $\gamma\gamma$ collider searches studied in [16, 17, 18, 19]. In this sense $\mathcal{O}_{\Phi 2}$ is "blind" to all these experiments and it can "see" an e^-e^+ collider only through the process $e^-e^+ \rightarrow ZH$ [6, 14].

Of course, the study of all these operators requires Higgs boson exchange or production processes. Such a study is relevant only in cases where the Higgs particle is sufficiently light and can therefore be produced at LEP2 or NLC. This is certainly possible if the NP scale is at the TeV range [20].

The subject of this paper is to study these NP effects on the processes $e^-e^+ \rightarrow ZH, \gamma H$. In SM, the process $e^-e^+ \rightarrow Z \rightarrow ZH$ is allowed at tree level (provided $m_H < \sqrt{s} - M_Z$) [21], while $e^-e^+ \rightarrow \gamma H$ is only possible at 1-loop level (if $m_H < \sqrt{s}$) [22, 23]. We use the same general framework as in [6, 24]. Here, in addition, we study in more

detail the angular distribution in $e^-e^+ \rightarrow Z f \bar{f} H$ and include the standard contribution to $e^-e^+ \rightarrow \gamma H$. For other recent works on these processes see [25, 26]. The complementary possibilities offered at higher energies for the first four of the above operators, where laser induced $\gamma\gamma$ collisions may be used to study the production of a single H or a boson pair, have been described in [18, 19, 16, 17].

The precision tests for $e^-e^+ \rightarrow ZH$ consist of measuring the angular distribution $d\sigma/d\cos\vartheta$ and the Z helicity density matrix elements through the analysis of the $Z \rightarrow f\bar{f}$ decay distribution; especially its dependence on the azimuthal angle ϕ_f . Here, ϑ is defined as the angle between the e^- beam and the Z direction in the e^-e^+ c.m. frame, while ϕ_f is the azimuthal angle of the charged fermion f with respect to the ZH production plane. In order to disentangle the contributions generated from the five operators above, we need suitable independent observables. We show that in addition to the Z angular distribution $d\sigma/d\cos\vartheta$, four azimuthal asymmetries determined respectively by the coefficients of the $\cos\phi_f$, $\sin\phi_f$, $\sin 2\phi_f$ and $\cos 2\phi_f$ terms of the $f\bar{f}$ plane distribution, will be useful for this search.

If the NP scale Λ_{NP} lies in the TeV range, the number of events at LEP2 will be too small to allow for such a detailed analysis. Thus, at LEP2 only $d\sigma/d\cos\vartheta$ will be measurable and will give a meaningful constraint to a combination of NP couplings (essentially the anomalous HZZ coupling). At NLC this study can be further pursued and a complete disentangling of the five couplings could then be expected, particularly if the results from $e^-e^+ \rightarrow ZH$ are combined with those from the processes studied in [16, 17, 18, 19].

The differential cross section for $e^-e^+ \rightarrow \gamma H$ provides also a very sensitive test of NP, in situations where the final photons are easily detected. In particular, if it happens that $m_H > 100 GeV$, this process may be the only way to produce H at LEP2. The operators studied through this process are \mathcal{O}_{UB} , \mathcal{O}_{UW} , $\overline{\mathcal{O}}_{UB}$, $\overline{\mathcal{O}}_{UW}$. Here, it is impossible to disentangle the CP -conserving pair (\mathcal{O}_{UB} , \mathcal{O}_{UW}) from the CP -violating one ($\overline{\mathcal{O}}_{UB}$, $\overline{\mathcal{O}}_{UW}$). Note also that the combination of the \mathcal{O}_{UB} and \mathcal{O}_{UW} couplings appearing in the γH angular distribution is different from the one appearing in ZH . Thus, the $e^-e^+ \rightarrow \gamma H$ differential cross section can be used to help disentangle \mathcal{O}_{UB} from \mathcal{O}_{UW} , without going through the difficult analysis of the Z spin density matrix. This later analysis would still be needed though to disentangle the CP -violating effects induced by $\overline{\mathcal{O}}_{UB}$ and $\overline{\mathcal{O}}_{UW}$.

In Section 2, we compute the helicity amplitudes for both $e^-e^+ \rightarrow ZH$ and $e^-e^+ \rightarrow \gamma H$ processes due to SM and NP contributions. The corresponding cross sections together with the other observables needed to discriminate among the effects of the five operators are discussed in Section 3 while the Z density matrix elements are derived in Appendices A, B. The results for the LEP2 and NLC conditions are presented and commented in the last Section 4, while in Section 5 we give our conclusions.

2 Anomalous Higgs couplings and $e^-e^+ \rightarrow ZH, \gamma H$ amplitudes

As discussed in the introduction and in previous papers [4, 6, 18, 16], there are only five $SU(2) \times U(1)$ gauge invariant $dim = 6$ operators relevant to $e^-e^+ \rightarrow ZH, \gamma H$. These consist of the four blind operators

$$\mathcal{O}_{UW} = \frac{1}{v^2}(\Phi^\dagger\Phi - \frac{v^2}{2}) \vec{W}^{\mu\nu} \cdot \vec{W}_{\mu\nu} \quad , \quad (1)$$

$$\mathcal{O}_{UB} = \frac{4}{v^2}(\Phi^\dagger\Phi - \frac{v^2}{2}) B^{\mu\nu} B_{\mu\nu} \quad , \quad (2)$$

$$\overline{\mathcal{O}}_{UW} = \frac{1}{v^2}(\Phi^\dagger\Phi) \vec{W}^{\mu\nu} \cdot \vec{\widetilde{W}}_{\mu\nu} \quad , \quad (3)$$

$$\overline{\mathcal{O}}_{UB} = \frac{4}{v^2}(\Phi^\dagger\Phi) B^{\mu\nu} \widetilde{B}_{\mu\nu} \quad , \quad (4)$$

and the "superblind" one²

$$\mathcal{O}_{\Phi 2} = 4\partial_\mu(\Phi^\dagger\Phi)\partial^\mu(\Phi^\dagger\Phi) \quad , \quad (5)$$

which is insensitive to LEP1 physics at the 1-loop level, but sensitive to the process $e^-e^+ \rightarrow ZH$ [4, 6, 14]. As usual, the vacuum expectation value of the Higgs field is denoted by $v = (G_F\sqrt{2})^{-1/2}$. The NP effective lagrangian determining the couplings of these operators is given by

$$\mathcal{L}_{NP} = d \mathcal{O}_{UW} + \frac{d_B}{4} \mathcal{O}_{UB} + \bar{d} \overline{\mathcal{O}}_{UW} + \frac{\bar{d}_B}{4} \overline{\mathcal{O}}_{UB} + \frac{f_{\Phi 2}}{v^2} \mathcal{O}_{\Phi 2} \quad . \quad (6)$$

The only effect of $\mathcal{O}_{\Phi 2}$ at the tree level is to induce a wave function renormalization to the Higgs field given by

$$Z_H = \frac{1}{1 + 8f_{\Phi 2}} \simeq 1 - 8f_{\Phi 2} \quad . \quad (7)$$

Here, as well as in the previous works [16, 17, 18, 19], we only consider tree level anomalous contributions and we restrict to cases where only one of the operators above acts each time. Thus, the $\mathcal{O}_{\Phi 2}$ contribution can only be studied in $e^-e^+ \rightarrow ZH$. In particular, in this framework there is no $\mathcal{O}_{\Phi 2}$ contribution to $e^-e^+ \rightarrow \gamma H$ or to the $\gamma\gamma$ and $e\gamma$ -Collider processes considered in [16, 17, 18, 19]. Contributions from $\mathcal{O}_{\Phi 2}$ to these later processes could arise at tree level only if terms bilinear in the anomalous couplings of two different operators were to be retained.

In the following, it will be convenient to introduce the definitions

$$d_{\gamma Z} = s_W c_W (d - d_B) \quad , \quad d_{ZZ} = d c_W^2 + d_B s_W^2 \quad , \quad d_{\gamma\gamma} = d s_W^2 + d_B c_W^2 \quad , \quad (8)$$

²Actually there exists also another superblind operator called $\mathcal{O}_{\Phi 3} = 8(\Phi^\dagger\Phi)^3$ which only gives an irrelevant Higgs mass renormalization and can therefore be neglected.

as well as the corresponding CP -violating ones for the \bar{d} , \bar{d}_B couplings defined in (6).

The invariant amplitude for $e^- e^+ \rightarrow Z_\tau H$ takes then the simple compact form (see also [25])

$$\begin{aligned}
F_{\lambda\tau}(e^- e^+ \rightarrow ZH) = & \frac{\lambda e g \sqrt{Z_H}}{M_W \sqrt{s}} \left(\frac{M_Z^2}{4c_W s_W} \chi(\lambda A_e - V_e) \left[(1 - \tau^2) \frac{k_0 \sin \vartheta}{M_Z} - \tau^2 \frac{\tau \cos \vartheta + \lambda}{\sqrt{2}} \right] \right. \\
+ & [d_{\gamma Z} + d_{ZZ} \frac{\chi}{4s_W c_W} (\lambda A_e - V_e)] [(1 - \tau^2) 2M_Z \sqrt{s} \sin \vartheta - \tau^2 k_0 \sqrt{2s} (\tau \cos \vartheta + \lambda)] \\
+ & \left. i[\bar{d}_{\gamma Z} + \bar{d}_{ZZ} \frac{\chi}{4s_W c_W} (\lambda A_e - V_e)] [\tau^2 k \sqrt{2s} (\cos \vartheta + \lambda \tau)] \right), \tag{9}
\end{aligned}$$

where τ is the Z helicity and $\lambda = \pm 1$ is the difference between the e^- and e^+ helicities. Moreover³, $\chi = s/(s - M_Z^2)$ while $V_f = 2t_f^{(3)} - 4Q_f s_W^2$, $A_f = 2t_f^{(3)}$ are the standard $Zf\bar{f}$ vector and axial couplings, with $t_f^{(3)}$ being the third component of the left-isospin of the fermion f . The quantities k , k_0 and ϑ are the momentum, energy and production angle of Z in the $e^- e^+$ c.m. frame respectively, with the z-axis defined by the e^- direction. The normalization of the invariant amplitude is such that

$$\frac{d\sigma(e^- e^+ \rightarrow ZH)}{d\cos \vartheta} = \frac{k}{64\pi s^{3/2}} \sum_{\lambda, \tau} |F_{\lambda\tau}|^2. \tag{10}$$

The first term in (9) gives the SM result, (apart of course from the $\mathcal{O}_{\Phi 2}$ contribution determined by the overall factor $\sqrt{Z_H}$). It involves the production of both transverse Z_T and longitudinal Z_L , but it is dominated by Z_L at high energies. The second term determines the CP -conserving anomalous contribution from \mathcal{O}_{UB} and \mathcal{O}_{UW} . It again involves production of both Z_T and Z_L , but it is Z_T now that dominates at high energies. The third term gives the CP -violating contribution which is purely Z_T and grows with the energy like the Z_T CP -conserving one. Concerning the overall factor $\sqrt{Z_H}$ in (9), we remark that according to the approximations explained above where only linear terms in the anomalous couplings were considered, we must substitute $Z_H \rightarrow 1$ whenever contributions from the last two terms in (9) are evaluated. We note also, that the CP -conserving (CP -violating) part of the amplitude in (9) satisfies

$$F_{++}(\cos \vartheta) = \pm F_{+-}(-\cos \vartheta), \tag{11}$$

$$F_{-+}(\cos \vartheta) = \pm F_{--}(-\cos \vartheta), \tag{12}$$

where the upper sign is for the CP -conserving part and the lower sign for the CP -violating one. These relations mean that $d\sigma/d\cos \vartheta$ for unpolarized e^\pm beams is symmetric under $\cos \vartheta \rightarrow -\cos \vartheta$; compare (19) below.

³ Of course close to the Z -pole we should replace $M_Z \rightarrow M_Z - i\Gamma_Z/2$.

We next turn to $e^- e^+ \rightarrow \gamma_\tau H$ for which we obtain

$$F_{\lambda\tau}^{(A)}(e^- e^+ \rightarrow \gamma H) = \frac{\lambda \, 2\sqrt{2} \, \pi\alpha}{s_W M_W \sqrt{s}} (s - m_H^2) \cdot \left\{ -(\tau \cos \vartheta + \lambda) [d_{\gamma\gamma} + d_{\gamma Z} \frac{\chi}{4s_W c_W} (\lambda A_e - V_e)] + i(\cos \vartheta + \tau\lambda) [\bar{d}_{\gamma\gamma} + \bar{d}_{\gamma Z} \frac{\chi}{4s_W c_W} (\lambda A_e - V_e)] \right\} , \quad (13)$$

$$F_{\lambda\tau}^{(SM)}(e^- e^+ \rightarrow \gamma H) = \frac{\lambda\alpha^2\sqrt{2}}{M_W s_W \sqrt{s}} (s - m_H^2) \cdot \left\{ (\tau \cos \vartheta + \lambda) [I_{\Delta G} + \frac{\chi}{4s_W^2} (V_e - \lambda A_e) I_{\Delta Z}] + \frac{s(1-\lambda)}{32s_W^2 M_W^2} [(\tau + \lambda)(1 + \cos \vartheta) I_W^+(\vartheta) + (\lambda - \tau)(1 - \cos \vartheta) I_W^-(\vartheta)] + \frac{s}{128s_W^2 M_W^2} (V_e^2 + A_e^2 - 2\lambda V_e A_e) [(\tau + \lambda)(1 + \cos \vartheta) I_Z^+(\vartheta) + (\lambda - \tau)(1 - \cos \vartheta) I_Z^-(\vartheta)] \right\} , \quad (14)$$

for the anomalous and the 1-loop SM contributions respectively. Here, ϑ is the c.m. angle of the final γ with respect to the e^- axis. The normalization of the amplitudes is the same as in the case of $e^- e^+ \rightarrow ZH$. In writing (13,14) we have again neglected tree-level contributions quadratic in the anomalous couplings, and also 1-loop contributions linear in the anomalous couplings. This implies that no contribution from $\mathcal{O}_{\Phi 2}$ should be included and thus no $\sqrt{Z_H}$ appears in (13,14).

The SM contribution to $e^- e^+ \rightarrow \gamma_\tau H$ is given by⁴ [22] in terms of the complex functions $I_{\Delta Z}(s)$, $I_{\Delta G}(s)$ describing the Z and γ exchange diagrams, and the functions $I_W^\pm(s, \vartheta)$, $I_Z^\pm(s, \vartheta)$ describing the W and Z boxes respectively. These functions are expressed by [22] as double integrals in the Feynman-parameter space⁵. The most difficult ones to calculate are $I_{\Delta Z}$, $I_{\Delta G}$, I_W^\pm , for which there exist singularity lines within the integration region for LEP2 energies and beyond. The numerical integration around these singularities can be done by using standard routines and Feynman's $i\epsilon$ prescription in order to separate principal-value and absorptive contributions. Such a separation should always be possible provided that these integrals are selected so that they can accept a

⁴A new analysis of the SM contribution has just appeared in [23]. The computation is done in a non linear gauge and the results are expressed in terms of a rather large number of dilogarithm functions. The numerical results for $\sigma(e^- e^+ \rightarrow \gamma H)$ are consistent with those of [22] but a little larger for $s \neq M_Z^2$, which gives a measure of the accuracy of the methods eventually used. This is not a problem for our purpose though, because the predicted SM rate seems unobservable in any case.

⁵See Eqs. (2.4a,4b,21,22,26,27), (A.3,4,8) in [22].

dispersive Mandelstam-type representation like the one satisfied by any Feynman amplitude.

We also note that [22]

$$I_W^-(s, \vartheta) = I_W^+(s, \pi - \vartheta) , \quad (15)$$

while

$$I_Z^-(s, \vartheta) = - I_Z^+(s, \pi - \vartheta) . \quad (16)$$

It then turns out that for LEP2 and NLC energies the Z -box contribution is rather small compared to the other ones, a result which is related to the fact that the relative integral has no absorptive part. This implies that the SM as well as the anomalous contribution to the amplitude for $e_\lambda^- e_\lambda^+ \rightarrow \gamma_\tau H$ satisfy approximately (11,12), which in turn leads to the conclusion that $d\sigma(e^- e^+ \rightarrow \gamma H)/d\cos\vartheta$ for unpolarized beams is essentially forward-backward symmetric.

3 Observables for $e^- e^+ \rightarrow Z_{(f\bar{f})} H$ and $e^- e^+ \rightarrow \gamma H$.

The Z spin density matrix in the helicity basis $\rho_{\tau\tau'}$ is calculated from the amplitude in (9) and given in Appendix A. Using that and assuming that the decay $Z \rightarrow f\bar{f}$ is standard, the angular distribution for the $f\bar{f}$ system in the Z rest frame is given by

$$\frac{d\sigma(e^- e^+ \rightarrow Z_{f\bar{f}} H)}{d\cos\vartheta d\Omega_f} = \frac{k B(Z \rightarrow f\bar{f})}{64\pi s \sqrt{s}} \sum_{\tau\tau'} \rho_{\tau\tau'} Q_{\tau\tau'} , \quad (17)$$

where $\Omega \equiv (\theta_f, \phi_f)$ are the angles of the fermion f in the Z -rest frame with the z-axis chosen along the Z momentum \mathbf{k} while the y-axis is along $\mathbf{e}^- \times \mathbf{k}$. The quantities $Q_{\tau\tau'}$ are given in Appendix B and $B(Z \rightarrow f\bar{f})$ is the Z branching ratio to $f\bar{f}$.

The first observable from $e^- e^+ \rightarrow ZH$ is the Z differential cross section obtained by integrating over the f -fermion solid angle

$$\frac{d\sigma(e^- e^+ \rightarrow ZH)}{d\cos\vartheta} = \frac{1}{B(Z \rightarrow f\bar{f})} \int d\Omega_f \frac{d\sigma(e^+ e^- \rightarrow H f\bar{f})}{d\cos\theta d\Omega_f} \quad (18)$$

which for unpolarized beams gives the explicit formula

$$\begin{aligned} \frac{d\sigma(e^- e^+ \rightarrow ZH)}{d\cos\vartheta} &= \frac{k}{64\pi s \sqrt{s}} (\rho_{++} + \rho_{--} + \rho_{--}) \\ &= \frac{\alpha^2 \pi k M_Z^2}{4s_W^2 c_W^2 s^{5/2}} Z_H \left\{ \frac{(1 - 4s_W^2 + 8s_W^4)}{4s_W^2} \chi^2 \left[\frac{2}{c_W^2} + \frac{k^2}{M_W^2} \sin^2 \vartheta \right] \right. \\ &\quad - \frac{4\chi k_0 \sqrt{s}}{s_W c_W M_Z^2} [2s_W^2 D_+ - (1 - 2s_W^2) D_-] \\ &\quad + \frac{4s}{M_Z^2} (D_+^2 + D_-^2) [2 + (1 + \cos^2 \vartheta) \frac{k^2}{M_Z^2}] \\ &\quad \left. + \frac{4sk^2}{M_Z^4} (1 + \cos^2 \vartheta) (\bar{D}_+^2 + \bar{D}_-^2) \right\} , \end{aligned} \quad (19)$$

where D_+ , D_- are given in (A.2,A.3) and correspondingly for the CP -violating couplings \overline{D}_+ , \overline{D}_- . As already noted, this expression is symmetric under the interchange $\vartheta \rightarrow \pi - \vartheta$.

An additional set of interesting four observables depending only on the four operators \mathcal{O}_{UB} , \mathcal{O}_{UW} , $\overline{\mathcal{O}}_{UB}$, $\overline{\mathcal{O}}_{UW}$ may be constructed by integrating (17) over $\cos \theta_f$ and the Z production angle ϑ . This gives

$$\begin{aligned} \frac{d\sigma(e^-e^+ \rightarrow Z_{f\bar{f}}H)}{d\phi_f} &\sim \int_{-1}^1 d\cos\vartheta \int_{-1}^1 d\cos\theta_f \sum_{\tau\tau'} \rho_{\tau\tau'} Q_{\tau\tau'} \\ &\sim [B + b_{13} \sin 2\phi_f + b_8 \cos 2\phi_f + b_{12} \sin \phi_f + b_{14} \cos \phi_f] , \end{aligned} \quad (20)$$

where b_{13} , b_8 , b_{12} and b_{14} depend only on s , and the four anomalous d -couplings defined in (6). The f_{Φ_2} coupling of \mathcal{O}_{Φ_2} is completely factored out and does not appear in these coefficients.

The b -quantities in (20) may be obtained by constructing suitable azimuthal asymmetries. To this end we integrate the above differential cross section with respect to ϕ_f over the regions $[0, \pi/4]$, $[\pi/4, \pi/2]$, $[\pi/2, 3\pi/4]$, $[3\pi/4, \pi]$, $[\pi, 5\pi/4]$, $[5\pi/4, 3\pi/2]$, $[3\pi/2, 7\pi/4]$, $[7\pi/4, 2\pi]$, calling the respective cross sections σ_{1a} , σ_{1b} , σ_{2a} , σ_{2b} , σ_{3a} , σ_{3b} , σ_{4a} , σ_{4b} , where the number in the index counts the quadrant in which ϕ_f lies. This way, we define the asymmetries

$$A_{13} = \frac{\sigma_{1a} + \sigma_{1b} + \sigma_{3a} + \sigma_{3b} - \sigma_{2a} - \sigma_{2b} - \sigma_{4a} - \sigma_{4b}}{\sigma} = \frac{2b_{13}}{\pi B} , \quad (21)$$

$$A_{12} = \frac{\sigma_{1a} + \sigma_{1b} + \sigma_{2a} + \sigma_{2b} - \sigma_{3a} - \sigma_{3b} - \sigma_{4a} - \sigma_{4b}}{\sigma} = \frac{2b_{12}}{\pi B} , \quad (22)$$

$$A_{14} = \frac{\sigma_{1a} + \sigma_{1b} + \sigma_{4a} + \sigma_{4b} - \sigma_{2a} - \sigma_{2b} - \sigma_{3a} - \sigma_{3b}}{\sigma} = \frac{2b_{14}}{\pi B} , \quad (23)$$

$$A_8 = \frac{\sigma_{1a} + \sigma_{2b} + \sigma_{3a} + \sigma_{4b} - \sigma_{1b} - \sigma_{2a} - \sigma_{3b} - \sigma_{4a}}{\sigma} = \frac{2b_8}{\pi B} , \quad (24)$$

where

$$\begin{aligned} B &= \frac{M_Z^2 \chi^2 (1 - 4s_W^2 + 8s_W^4)}{4s_W^2 c_W^2} [2M_Z^2 + k_0^2] - \frac{6M_Z^2 k_0 \sqrt{s} \chi}{s_W c_W} [2s_W^2 D_+ - (1 - 2s_W^2) D_-] \\ &\quad + 4s(M_Z^2 + 2k_0^2)(D_+^2 + D_-^2) + 8sk^2(\overline{D}_+^2 + \overline{D}_-^2) , \end{aligned} \quad (25)$$

$$b_{13} = -\frac{k\sqrt{s}M_Z^2\chi}{s_W c_W} (2s_W^2 \overline{D}_+ - (1 - 2s_W^2) \overline{D}_-) + 4kk_0s(D_+ \overline{D}_+ + D_- \overline{D}_-) , \quad (26)$$

$$\begin{aligned} b_{12} &= -\frac{9\pi^2 M_Z}{16} \left(\frac{V_f A_f}{V_f^2 + A_f^2} \right) \left[4sk(D_- \overline{D}_- - D_+ \overline{D}_+) \right. \\ &\quad \left. + \frac{\chi k k_0 \sqrt{s}}{s_W c_W} [2s_W^2 \overline{D}_+ + (1 - 2s_W^2) \overline{D}_-] \right] , \end{aligned} \quad (27)$$

$$\begin{aligned} b_{14} &= -\frac{9\pi^2 M_Z}{16} \left(\frac{V_f A_f}{V_f^2 + A_f^2} \right) \left[\frac{M_Z^2 (1 - 4s_W^2) \chi^2 k_0}{4s_W^2 c_W^2} \right. \\ &\quad \left. + \frac{\sqrt{s} \chi}{s_W c_W} (k_0^2 + M_Z^2) [2s_W^2 D_+ + (1 - 2s_W^2) D_-] + 4sk_0(D_-^2 - D_+^2) \right] , \end{aligned} \quad (28)$$

$$\begin{aligned}
b_8 = & \frac{M_Z^4(1 - 4s_W^2 + 8s_W^4)}{8s_W^2 c_W^2} \chi^2 - \frac{M_Z^2 \chi k^0 \sqrt{s}}{s_W c_W} (2s_W^2 D_+ - (1 - 2s_W^2) D_-) \\
& + 2sk_0^2(D_+^2 + D_-^2) - 2sk^2(\overline{D}_+^2 + \overline{D}_-^2) \quad .
\end{aligned} \tag{29}$$

The above way for measuring these asymmetries assumes of course that the whole ϕ_f range is covered. Otherwise, these asymmetries should be measured by fitting the ϕ_f distribution using (20).

Turning now to the differential cross section for $e^-e^+ \rightarrow \gamma H$, assuming unpolarized beams and neglecting the SM contribution we get

$$\begin{aligned}
\frac{d\sigma(e^-e^+ \rightarrow \gamma H)}{d\cos\vartheta} = & \frac{\pi\alpha^2}{8M_W^2 s_W^2} \left(1 - \frac{m_H^2}{s}\right)^3 (1 + \cos^2\vartheta) \cdot \\
& \left\{ (d^2 + \overline{d}^2) \left[2s_W^4 + \chi(1 - 4s_W^2)s_W^2 + \chi^2\left(\frac{1}{4} - s_W^2 + 2s_W^4\right) \right] \right. \\
& + (d_B^2 + \overline{d}_B^2) \left[2c_W^4 - \chi(1 - 4s_W^2)c_W^2 + \chi^2\left(\frac{1}{4} - s_W^2 + 2s_W^4\right) \right] \\
& + (dd_B + \overline{d}\overline{d}_B) \left[4s_W^2 c_W^2 + \chi(1 - 4s_W^2)(1 - 2s_W^2) \right. \\
& \left. \left. - 2\chi^2\left(\frac{1}{4} - s_W^2 + 2s_W^4\right) \right] \right\} \quad .
\end{aligned} \tag{30}$$

We note though that in the numerical calculations presented below we have used the complete expressions given by the amplitudes in (13,14) which include both the SM and the anomalous contributions.

4 Analysis at LEP2 and NLC.

Before discussing the prospects for detecting NP at LEP2 and NLC, let us first describe what we can reasonably expect for the magnitude of the anomalous couplings appearing in the effective NP Lagrangian in (6). The most straightforward way to estimate the possible magnitude of these coupling is by using the unitarity relations. For the operators \mathcal{O}_{UB} , \mathcal{O}_{UW} , $\overline{\mathcal{O}}_{UB}$, $\overline{\mathcal{O}}_{UW}$, \mathcal{O}_{Φ^2} these relations are already known [27, 28, 15]. Calling Λ_{NP} the operator dependent NP scale where the related forces become strong, these unitarity relations may be written as⁶ [19]

$$d \simeq \frac{104.5 \left(\frac{M_W}{\Lambda_{NP}}\right)^2}{1 + 6.5 \left(\frac{M_W}{\Lambda_{NP}}\right)}, \text{ for } d > 0,$$

⁶These unitarity relations are obtained by making simple fits to the expression for the maximum eigenvalue of the partial wave transition matrix. For the operators in (1)-(4), the fits in [27, 28, 15] were occasionally valid only up to $3TeV$. Here we give better ones valid for any $\Lambda_{NP} \gtrsim 1TeV$.

$$d \simeq -\frac{104.5 \left(\frac{M_W}{\Lambda_{NP}}\right)^2}{1 - 4 \left(\frac{M_W}{\Lambda_{NP}}\right)^2}, \text{ for } d < 0, \quad (31)$$

$$d_B \simeq \frac{195.8 \left(\frac{M_W}{\Lambda_{NP}}\right)^2}{1 + 200 \left(\frac{M_W}{\Lambda_{NP}}\right)^2}, \text{ for } d_B > 0, \\ d_B \simeq -\frac{195.8 \left(\frac{M_W}{\Lambda_{NP}}\right)^2}{1 + 50 \left(\frac{M_W}{\Lambda_{NP}}\right)^2}, \text{ for } d_B < 0, \quad (32)$$

$$|\bar{d}| \simeq \frac{104.5 \left(\frac{M_W}{\Lambda_{NP}}\right)^2}{1 + 3 \left(\frac{M_W}{\Lambda_{NP}}\right)^2}, \quad (33)$$

$$|\bar{d}_B| \simeq \frac{195.8 \left(\frac{M_W}{\Lambda_{NP}}\right)^2}{1 + 100 \left(\frac{M_W}{\Lambda_{NP}}\right)^2}. \quad (34)$$

Applying (31-34) for $\Lambda_{NP} = 1TeV$, we get $d \simeq 0.4$ or $-1.$, $d_B \simeq 0.6$ or $-1.$, $|\bar{d}| \simeq 0.5$, $|\bar{d}_B| \simeq 0.8$ which give an estimate of the possible largest values for these couplings. Similar indications are also obtained from an 1-loop analysis of the LEP1 precision measurements [4, 6].

For the superblind operator $\mathcal{O}_{\Phi 2}$, a similar as in [27, 28, 15] unitarity analysis derives its strongest result from the $J = 0$ (partial wave) transition amplitudes involving the channels $|HH\rangle$, $|W^-W^+ LL\rangle$, $|ZZ LL\rangle$. Such a study gives unitarity saturation for

$$\left| \frac{f_{\Phi 2}}{(1 + 8 f_{\Phi 2})^2} \right| \simeq \frac{1}{a_w}, \quad (35)$$

where

$$a_w = \frac{\alpha\sqrt{3}}{4s_W^2} \frac{\Lambda_{NP}^2}{M_W^2}. \quad (36)$$

Solving (35), we obtain that for $\Lambda_{NP} < 3.7TeV$ (*i.e.* $0 < a_w < 32$) there is no unitarity constrain for $f_{\Phi 2} > 0$; while for $f_{\Phi 2} < 0$ we get

$$f_{\Phi 2} \simeq \frac{-16 - a_w + \sqrt{a_w(a_w + 32)}}{128}. \quad (37)$$

On the contrary, for $\Lambda_{NP} > 3.7TeV$ (*i.e.* $a_w > 32$) we get

$$f_{\Phi 2} \simeq \frac{-16 + a_w - \sqrt{a_w(a_w - 32)}}{128} \quad \text{for } f_{\Phi 2} > 0, \\ f_{\Phi 2} \simeq \frac{-16 - a_w + \sqrt{a_w(a_w + 32)}}{128} \quad \text{for } f_{\Phi 2} < 0, \quad (38)$$

which for $\Lambda_{NP} \gg 3.7 TeV$ gives

$$|f_{\Phi 2}| \simeq 75 \frac{M_W^2}{\Lambda_{NP}^2} . \quad (39)$$

Thus, if *e.g.* $|f_{\Phi 2}| \simeq 0.004$, then the $\mathcal{O}_{\Phi 2}$ -forces become strong at $\Lambda_{NP} = 10 TeV$, and therefore a related NP should appear by the time we reach this energy scale.

After establishing our expectations on how large these NP couplings could be, we turn to the process $e^-e^+ \rightarrow HZ_{(f\bar{f})}$. Its total cross section as a function of the e^-e^+ energy is shown in Fig.1 assuming $m_H = 80 GeV$. This value has been chosen optimistically, hoping that the Higgs will be produced at LEP2 through $e^-e^+ \rightarrow ZH$. In this figure, we present results for various values of the d and d_B couplings, indicating also the corresponding NP scale they correspond to. Identical results are of course also obtained for the same values of the CP -violating couplings \bar{d} and \bar{d}_B respectively.

The HZ angular distribution is mainly sensitive to $f_{\Phi 2}$ through the renormalization factor Z_H and to the combination $d_{ZZ} = dc_W^2 + d_B s_W^2$. Figs.2a,b,c show this sensitivity for the three nominal LEP2 energies, 175, 192 and 205 GeV . Assuming an integrated luminosity of 500, 300 and 300 pb^{-1} respectively, one expects about two hundred raw events; this number being then reduced by the H and Z detection. Because of this, we cannot expect to measure this cross section at LEP2 with an accuracy better than about 10%. Assuming that only one NP operator acts each time, we then deduce an observability limit $|f_{\Phi 2}| \simeq 0.01$ corresponding to $\Lambda_{NP} \simeq 6 - 7 TeV$, or an observability limit $|d| \simeq 0.015$ ($|d_B| \simeq 0.05$) corresponding to $\Lambda_{NP} \simeq 6 - 7 TeV$ ($\Lambda_{NP} \simeq 5 TeV$) for $m_H \simeq 80 GeV$. This is not so bad for a first exploration of the Higgs sector! However, with such a number of events it is not conceivable to make a meaningful analysis of the Z decay distribution in order to disentangle the various NP operators.

At higher energies, with the designed luminosities of NLC, the number of events is increasing as well as the sensitivity to anomalous couplings. For example at 1 TeV , with 80 fb^{-1} per year, the SM rate gives one thousand events per year. One can then expect a measurement of the cross section with a 3% accuracy. The implied sensitivities to the various couplings become $|f_{\Phi 2}| \simeq 0.004$, $|d| \simeq 0.005$ and $|d_B| \simeq 0.015$ corresponding to NP scales of 10, 11 and 9 TeV respectively; compare Fig.1 and Fig.3. Moreover, with such a number of events, azimuthal asymmetries could be used in order to disentangle the various d -type couplings.

As noted already, there are four kinds of such asymmetries. We first discuss A_{14} and A_{12} which are shown in Figs.4,5. These asymmetries depend on the flavour of the fermion f to which Z decays and are mostly interesting for the $Z \rightarrow b\bar{b}$ case. From Figs.4,5 it looks possible that the sensitivities to d and d_B could reach the percent level. Note also that A_{14} , A_{12} depend mainly on the combination $d_{\gamma Z} = s_W c_W (d - d_B)$ and on its CP -violating partner $\bar{d}_{\gamma Z}$. Thus, the illustrations made for d (\bar{d}) apply also to $-d_B$, ($-\bar{d}_B$). The asymmetry A_{13} shown in Fig.6 does not depend on the type of the fermion f but it is sensitive to the CP -violating combination \bar{d}_{ZZ} ; (compare (8)). Thus, sensitivities to this coupling at the percent level should be possible using this asymmetry. Note that in this case the sensitivities to d_B and d are related by $d_B \simeq dc_W^2/s_W^2$. Finally the asymmetry

A_8 shown in Fig.7, is also mainly sensitive to d_{ZZ} and independent of the flavour of the f fermion. Consequently, the differential cross section for $e^-e^+ \rightarrow ZH$, together with the above asymmetries, provide considerable information for disentangling the aforementioned five relevant anomalous couplings at the percent level. It follows that NP scales of the order of a few TeV could be searched for this way.

Further information on the above four d -type couplings, can be obtained from the differential cross section for the process $e^-e^+ \rightarrow \gamma H$. At SM this cross section is unobservably small, but it is very sensitive to the four NP interactions. Thus, the differential cross section could become observable if non negligible anomalous interactions occur, which according to (30) imply an angular distribution of the form $1 + \cos^2 \vartheta$ [29]. If $m_H \lesssim 90 GeV$, this process is allowed already at LEP1, leading to a rather low energy photon together with a Higgs particle decaying mainly to $b\bar{b}$. The background to this process comes mainly from final state radiation in the $Z \rightarrow b\bar{b}$ process. A discussion of this problem has been given in [30, 29]. On the basis of this we conclude that for *e.g.* $m_H \sim 80 GeV$, we would need about a hundred events in order to obtain a visible signal over a background of about 10^{+7} Z . This then means that $\sigma(e^-e^+ \rightarrow \gamma H) \gtrsim 0.3 pb$ is required, which is at least a factor 100 above the SM rate and requires anomalous Higgs couplings satisfying $|d| \gtrsim 0.1$ or $|d_B| \gtrsim 0.1$. So these (rough) constraints leave room for the analysis of the $e^-e^+ \rightarrow HZ$ process at LEP2 that we proposed above.

One can then look for the $e^-e^+ \rightarrow \gamma H$ process at LEP2 where the Higgs is associated to very energetic photons, for which there should be no such background. As a first illustration we plot in Fig.8a the photon angular distribution in terms of $|\cos \vartheta|$, for $m_H = 80 GeV$ and e^-e^+ c.m. energy $192 GeV$. There are various remarks to be made now. Thus, for SM we find $\sigma(e^-e^+ \rightarrow \gamma H) \simeq 0.16 fb$, which is consistent with the result of⁷ [23]. As we see from this figure, a much higher cross section will appear if an anomalous interaction is present. Because of this and demanding a few events, one sees that a sensitivity to $|d| \simeq 0.05$ or $|d_B| \simeq 0.025$ is possible for $m_H \sim 80 GeV$, which means testing NP scales of 3 and 7 TeV respectively. These later sensitivities come from (d, d_B) combinations that are different from those appearing in HZ production, which provides a welcome help for disentangling these two operators. Since $m_H = 80 GeV$ is far below the LEP2 c.m. energy, we observe that the cross sections presented in Fig.8a remain true also for the other LEP2 nominal energies, namely 175 and 205 GeV . Finally we should remark that the difference between the predictions for the various cross sections corresponding to opposite signs of any anomalous coupling, gives a measure of the magnitude of the interference contribution between the standard and anomalous terms. It can therefore be seen that *e.g.* in Fig.8a, this difference is much smaller than the difference in Figs.2a,b,c.

The very interesting thing concerning $e^-e^+ \rightarrow \gamma H$ is that it allows for a similar sensitivity on d or d_B , even in the case that the Higgs is considerably heavier. This can be seen from Fig.8b where the angular distribution for *e.g.* $m_H = 120 GeV$ and a total e^-e^+ energy of 192 GeV , is presented. It can also be seen there, that $\sigma(e^-e^+ \rightarrow \gamma H) \sim 13 fb$ for $|d| \sim 0.1$, while the SM expectation is about 0.084 fb [23].

⁷It is amusing to state that the tools for the numerical calculations used here are rather primitive compared to [31] employed in [23].

For a 1TeV NLC, Fig.9a,b show a sensitivity to $|d| \simeq 0.005$ and $|d_B| \simeq 0.0025$ corresponding to NP scales of 11 and 22 TeV respectively. In these figures we have used for illustration $m_H = 80\text{GeV}$, but of course similar results would have been expected for any $m_H \ll 1\text{TeV}$. Note also that at such an energy, the SM differential cross section is somewhat enhanced in the forward and backward regions, while the total cross section reaches the 0.014fb level.

5 Conclusions

We have studied the sensitivity to NP of the processes $e^-e^+ \rightarrow ZH$ and γH that are observable at LEP2 and higher energy e^-e^+ colliders. Our analysis is concentrated on the residual NP effects described by the $\text{dim} = 6$ $SU(2) \times U(1)$ gauge invariant operators \mathcal{O}_{UB} , \mathcal{O}_{UW} , $\overline{\mathcal{O}}_{UB}$, $\overline{\mathcal{O}}_{UW}$, $\mathcal{O}_{\Phi 2}$, which only affect the Higgs couplings to themselves and to gauge bosons. We have given explicit analytic expressions for the helicity amplitudes and the angular distributions for HZ and $H\gamma$ as well as Z the spin density matrix elements and azimuthal asymmetries in $Z \rightarrow f\bar{f}$ decays.

We first performed an analysis for the LEP2 conditions, using $M_H = 80\text{GeV}$ as an illustration. From the study of $d\sigma/d\cos\vartheta$ in $e^-e^+ \rightarrow ZH$, a sensitivity to $\mathcal{O}_{\Phi 2}$ is expected up to a NP scale of 6-7 TeV , and to \mathcal{O}_{UB} and \mathcal{O}_{UW} up to scales of 5 and 7 TeV respectively. For the process $e^-e^+ \rightarrow \gamma H$ the SM rate is unobservable, but the anomalous interactions we consider could strongly enhance it. At LEP1 the background is too strong to allow for the observability of this process if $m_H \sim 80\text{GeV}$ and the NP scales are at the aforementioned level. At LEP2, where the background is reduced, the observation of a few events would imply the presence of NP due to \mathcal{O}_{UB} or \mathcal{O}_{UW} effects at 7 or 3 TeV respectively. Furthermore, a comparison between the two processes $e^-e^+ \rightarrow ZH$ and $e^-e^+ \rightarrow \gamma H$ could be used for disentangling the effects of the operators \mathcal{O}_{UB} and \mathcal{O}_{UW} that are involved in different combinations.

The $e^-e^+ \rightarrow \gamma H$ process is also particularly interesting at LEP2 energies, as it may allow for the production and study of a Higgs particle with $m_H \gtrsim 100\text{GeV}$, which would not be possible through $e^-e^+ \rightarrow ZH$. Thus, for *e.g.* $m_H = 120\text{GeV}$ and a total e^-e^+ energy of 192GeV , we should be able to observe NP effects at scales similar to those observable in the $m_H \sim 80\text{GeV}$ case.

At NLC in the 1TeV range, the sensitivity increases due to the s -dependence and the larger luminosity. Studying therefore $e^-e^+ \rightarrow ZH$, a complete disentangling of the five operators can be envisaged by using in addition the four azimuthal asymmetries associated to the $\cos\phi_f$, $\sin\phi_f$, $\sin 2\phi_f$ and $\cos 2\phi_f$ distributions. This disentangling should be achievable down to the percent level for the NP couplings, implying sensitivities to NP scales of the order of 10, 8 and 12 TeV for $\mathcal{O}_{\Phi 2}$, \mathcal{O}_{UB} and \mathcal{O}_{UW} respectively. The $e^-e^+ \rightarrow \gamma H$ process could feel \mathcal{O}_{UB} and \mathcal{O}_{UW} up to scales of 20 and 12 TeV . In this respect the disentangling may be further helped by comparing with the analyses of other bosonic processes like *e.g.* boson pair production [18, 19] and single Higgs boson production in $\gamma\gamma$ collisions [16, 17].

In conclusion, if m_H is small enough, we can expect a remarkable first exploration of the Higgs sector at LEP2, while at NLC a detail study of the NP properties should be made possible for a wider range of m_H and Λ_{NP} scales.

Acknowledgements: We would like to thank Jorge Romão and Wayne Repko for communications concerning Refs. [22, 23].

Appendix A : Z spin density matrix elements in $e^-e^+ \rightarrow ZH$

From the helicity amplitudes of Section 2 one computes the (un-normalized) Z density matrix elements

$$\rho_{\tau\tau'} = \rho_{\tau'\tau}^* = \sum_{\lambda=\pm 1} F_{\lambda\tau} F_{\lambda\tau'}^* . \quad (\text{A.1})$$

It is convenient to define the following left-handed and right-handed combinations of couplings:

$$D_+ = s_W c_W \left[d(1 - \chi) - d_B(1 + \chi \frac{s_W^2}{c_W^2}) \right] , \quad (\text{A.2})$$

$$D_- = s_W c_W \left[d \left(1 + \chi \left(\frac{1}{2s_W^2} - 1 \right) \right) - d_B \left(1 + \chi \left(\frac{1}{2c_W^2} - 1 \right) \right) \right] , \quad (\text{A.3})$$

and similarly for the CP -violating couplings. As before, $\chi = s/(s - M_Z^2)$. Using these definitions and denoting by Z_H the H field wave function renormalization induced by $\mathcal{O}_{\Phi 2}$, the Z density matrix elements become

$$\begin{aligned} \rho_{++}(\vartheta) = & Z_H \frac{e^2 g^2 (1 + \cos^2 \vartheta)}{2s M_W^2} \left\{ M_Z^4 \chi^2 \frac{(1 - 4s_W^2 + 8s_W^4)}{4s_W^2 c_W^2} \right. \\ & + \frac{2M_Z^2 \chi k_0 \sqrt{s}}{s_W c_W} [(1 - 2s_W^2)D_- - 2s_W^2 D_+] \\ & \left. + 4k_0^2 s (D_+^2 + D_-^2) + 4k^2 s (\overline{D}_+^2 + \overline{D}_-^2) \right\} \\ & - Z_H \frac{e^2 g^2 \cos \vartheta}{s M_W^2} \left\{ M_Z^4 \chi^2 \frac{(1 - 4s_W^2)}{4s_W^2 c_W^2} + \frac{2M_Z^2 \chi k_0 \sqrt{s}}{s_W c_W} [(1 - 2s_W^2)D_- + 2s_W^2 D_+] \right. \\ & \left. + 4k_0^2 s (D_-^2 - D_+^2) + 4k^2 s (\overline{D}_-^2 - \overline{D}_+^2) \right\} , \end{aligned} \quad (\text{A.4})$$

$$\rho_{--}(\vartheta) = \rho_{++}(\pi - \vartheta) , \quad (\text{A.5})$$

$$\begin{aligned} \rho_{00}(\vartheta) = & Z_H \frac{e^2 g^2 \sin^2 \vartheta}{s c_W^2} \left\{ \frac{k_0^2 \chi^2}{4c_W^2 s_W^2} (1 - 4s_W^2 + 8s_W^4) \right. \\ & \left. - \frac{2\sqrt{s} k_0 \chi}{c_W s_W} [2s_W^2 D_+ - (1 - 2s_W^2)D_-] + 4s [D_+^2 + D_-^2] \right\} , \end{aligned} \quad (\text{A.6})$$

$$\begin{aligned} \rho_{0+}(\vartheta) = & Z_H \frac{e^2 g^2 \sin \vartheta}{\sqrt{2} M_W^2 s} \left\{ \frac{M_Z^4 \chi^2 k_0}{4s_W^2 c_W M_W} [1 - 4s_W^2 - (1 - 4s_W^2 + 8s_W^4) \cos \vartheta] \right. \\ & + \frac{M_Z^3 \sqrt{s} \chi}{s_W c_W} \left(1 + \frac{k_0^2}{M_Z^2} \right) [(1 - 2s_W^2)(1 - \cos \vartheta)D_- + 2s_W^2(1 + \cos \vartheta)D_+] \\ & + 4s M_Z k_0 [(1 - \cos \vartheta)D_-^2 - (1 + \cos \vartheta)D_+^2] \\ & + 4ik M_Z s [D_- \overline{D}_- (1 - \cos \vartheta) - D_+ \overline{D}_+ (1 + \cos \vartheta)] \\ & \left. + i \frac{k k_0 \sqrt{s} M_Z \chi}{c_W s_W} [(1 - \cos \vartheta)(1 - 2s_W^2)\overline{D}_- + 2s_W^2(1 + \cos \vartheta)\overline{D}_+] \right\} , \end{aligned} \quad (\text{A.7})$$

$$\rho_{0-}(\vartheta) = \rho_{0+}^*(\pi - \vartheta) \quad , \quad (\text{A.8})$$

$$\begin{aligned} \rho_{+-}(\vartheta) = & Z_H \frac{e^2 g^2 \sin^2 \vartheta}{2M_W^2 s} \left\{ M_Z^4 \chi^2 \frac{(1 - 4s_W^2 + 8s_W^4)}{4s_W^2 c_W^2} \right. \\ & + \frac{2M_Z^2 \chi k_0 \sqrt{s}}{s_W c_W} [(1 - 2s_W^2)D_- - 2s_W^2 D_+] \\ & + 4k_0^2 s(D_+^2 + D_-^2) - 4k^2 s(\overline{D}_+^2 + \overline{D}_-^2) \\ & - \frac{2ik\sqrt{s}M_Z^2 \chi}{s_W c_W} [(1 - 2s_W^2)\overline{D}_- - 2s_W^2 \overline{D}_+] \\ & \left. - 8ikk_0 s(D_+ \overline{D}_+ + D_- \overline{D}_-) \right\} . \quad (\text{A.9}) \end{aligned}$$

Appendix B : Z decay distributions and projectors

Assuming that the $Z \rightarrow f\bar{f}$ amplitude is standard, the angular distribution of the $f\bar{f}$ system in the Z rest frame is determined according to (17) by Z density matrix $\rho_{\tau\tau'}$ in the helicity basis and the decay elements $Q_{\tau\tau'}$. Using the notation introduced in Sect.3 and the definitions immediately after (9) we have

$$Q_{\pm\pm} = \frac{3}{16\pi} \left(1 + \cos^2 \theta_f \mp \frac{4A_f V_f}{A_f^2 + V_f^2} \cos \theta_f \right) , \quad (\text{B.1})$$

$$Q_{00} = \frac{3}{8\pi} \sin^2 \theta_f , \quad (\text{B.2})$$

$$Q_{\pm\mp} = \frac{3}{16\pi} \sin^2 \theta_f e^{\pm 2i\phi_f} , \quad (\text{B.3})$$

$$Q_{\pm 0} = Q_{0\pm}^* = \frac{3\sqrt{2}}{16\pi} \sin \theta_f e^{\pm i\phi_f} \left[\pm \cos \theta_f - \frac{2A_f V_f}{A_f^2 + V_f^2} \right] . \quad (\text{B.4})$$

The associated $\Lambda_{\tau\tau'}^Z$ projectors defined by

$$\int Q_{\tau\tau'}(\theta_f, \phi_f) \Lambda_{\mu\mu'}^Z(\theta_f, \phi_f) d\Omega_f = \delta_{\tau\mu} \delta_{\tau'\mu'} , \quad (\text{B.5})$$

are

$$\Lambda_{00}^Z = 2 - 5 \cos^2 \theta_f , \quad (\text{B.6})$$

$$\Lambda_{\pm\pm}^Z = \frac{1}{2} \left[5 \cos^2 \theta_f \mp \frac{V_f^2 + A_f^2}{A_f V_f} \cos \theta_f - 1 \right] , \quad (\text{B.7})$$

$$\Lambda_{\pm\mp}^Z = 2e^{\mp 2i\phi_f} , \quad (\text{B.8})$$

$$\Lambda_{\pm 0}^Z = \Lambda_{0\pm}^{Z*} = -\frac{2\sqrt{2}}{3\pi} \left[\frac{V_f^2 + A_f^2}{V_f A_f} \mp 8 \cos \theta_f \right] e^{\mp i\phi_f} . \quad (\text{B.9})$$

The Z density matrix elements can be extracted from a given angular distribution by integrating over the final fermion solid angle using these projectors according to

$$\rho_{\tau\tau'}(\vartheta) = \frac{64\pi s\sqrt{s}}{kB(Z \rightarrow f\bar{f})} \int d\Omega_f \frac{d\sigma(e^+e^- \rightarrow Hf\bar{f})}{d\cos\vartheta d\Omega_f} \Lambda_{\tau\tau'}^Z . \quad (\text{B.10})$$

References

- [1] J. Gunion, H. Haber, G. Kane and S. Dawson, The Higgs Hunter's guide, Addison-Wesley, Reading 1990.
- [2] A. Djouadi, Int. J. Mod. Phys. **A10** (1995) 1.
- [3] A. De Rújula, M.B. Gavela, P. Hernandez and E. Masso, Nucl. Phys. **B384** (1992) 3.
- [4] K. Hagiwara, S. Ishihara, R. Szalapski and D. Zeppenfeld, Phys. Lett. **B283** (1992) 353 and Phys. Rev. **D48** (1993) 2182.
- [5] D. Schaile, presented at the 27th Int. Conf. on High Energy Phys., Glasgow, (1994).
- [6] K. Hagiwara, R. Szalapski and D. Zeppenfeld, Phys. Lett. **B318** (1993) 155.
- [7] G.J. Gounaris, F.M. Renard and C. Verzegnassi, hep-ph/9501362, Phys. Rev. **D52** (1995) 451.
- [8] K.J.F. Gaemers and G.J. Gounaris, Z. Phys. **C1** (1979) 259; K. Hagiwara, R. Peccei, D. Zeppenfeld and K. Hikasa, Nucl. Phys. **B282** (1987) 253.
- [9] M. Bilenky, J.L. Kneur, F.M. Renard and D. Schildknecht, Nucl. Phys. **B409** (1993) 22 and **B419** (1994) 240.
- [10] G.J. Gounaris et al, in Proc. of the Workshop on e^+e^- Collisions a 500 GeV: The Physics Potential, DESY 92-123B(1992), p.735, ed. P.Zerwas; M.Bilenky et al, **B419** (1994) 240.
- [11] M. Kuroda, F.M. Renard and D. Schildknecht, Z. Phys. **C40** (1988) 575; T.L. Barklow, SLAC-PUB-5808 (1992).
- [12] P.M.Zerwas, DESY 93-112, Aug.1993; Proc. of the Workshop on e^+e^- Collisions a 500 GeV: The Physics Potential, DESY 92-123A+B+C(1992), ed. P.Zerwas;
- [13] G.Belanger and F.Boudjema, Ref. [12], p.783; S.Y.Choi and F.Schrempp, Ref. [12], p.793.
- [14] G.J. Gounaris, F.M. Renard and G. Tsirigoti, Phys. Lett. **B338** (1994) 51.
- [15] G.J. Gounaris, F.M. Renard and G. Tsirigoti, Phys. Lett. **B350** (1995) 212.
- [16] G.J. Gounaris, J. Layssac and F.M. Renard, Z. Phys. **C65** (254) 1995.
- [17] G.J. Gounaris and F.M. Renard, hep-ph/9505429 Montpellier and Thessaloniki preprint PM/95-20, THES-TP 95/07, to appear in Zeit. f. Physik.
- [18] G.J. Gounaris and F.M. Renard, Phys. Lett. **B326** (1994) 131.

- [19] G.J. Gounaris, J. Layssac and F.M. Renard, hep-ph/9505430 Montpellier and Thessaloniki preprint PM/95-11, THES-TP 95/06, to appear in Zeit. f. Physik.
- [20] G. Altarelli and G. Isidori, CERN-TH 7351/94; M. Quirós, CERN-TH/95-197, hep-ph/9507317.
- [21] J. Ellis, M.K. Gaillard and D.V. Nanopoulos, Nucl. Phys. **B106** (1976) 292; B.W. Lee, C. Quigg and H.B. Thacker, Phys. Rev. **D16** (1977) 1519; J.D. Bjorken, Proc. Sum. Inst. Part. Phys., SLAC Rep. 198(1976); B.L. Ioffe and V.A. Khoze, Sov.J.Part.Nucl. 9(1978)50.
- [22] A. Barroso, J. Pulido and J.C. Romão, Nucl. Phys. **B267** (1986) 509.
- [23] A. Abbasabadi, D.Bowser-Chao, D.A. Dicus and W.W. Repko, preprint MSUHEP-41012, hep-ph/9507463.
- [24] V. Barger, F.Cheung, A. Djouadi, B.A. Kniehl and P.M. Zerwas, Phys. Rev. **D49** (1994) 79; M. Krämer, J. Kühn, M.L. Stong and P.M. Zerwas, Z. Phys. **C64** (1994) 21.
- [25] K. Hagiwara and M.L. Stong, Z. Phys. **C62** (1994) 99.
- [26] J.P. Ma and B.H.J. McKellar, Phys. Rev. **D52** (1995) 22.
- [27] G.J. Gounaris, J. Layssac and F.M. Renard, Phys. Lett. **B332** (1994) 146.
- [28] G.J. Gounaris, J. Layssac, J.E. Paschalis and F.M. Renard, Z. Phys. **C66** (1995) 619.
- [29] P. Mättig, CERN-PPE/95-081 (unpublished).
- [30] Report of the working group on High Luminosities at LEP, CERN 91-02 (1991), p.88.
- [31] D.A. Dicus and C. Kao, LOOP, a FORTRAN program for doing loop integrations of 1,2,3 and 4 point functions with momenta in the numerator, 1991 (unpublished); G.J. van Oldenborgh and J.A.M. Vermaseren, Z. Phys. **C46** (1990) 425.

Figure Captions

Fig.1 Cross section for $e^+e^- \rightarrow HZ$ versus e^+e^- total energy for $m_H = 80\text{GeV}$. SM and NP contributions due to \mathcal{O}_{UB} , \mathcal{O}_{UW} , and $\mathcal{O}_{\Phi 2}$.

Fig.2 Angular distribution of $e^+e^- \rightarrow HZ$ versus $|\cos\vartheta|$ at three LEP2 energies (a) 175 GeV, (b) 192 GeV, (c) 205 GeV, for $m_H = 80\text{GeV}$, SM and NP contributions due to \mathcal{O}_{UB} , \mathcal{O}_{UW} , and $\mathcal{O}_{\Phi 2}$. The number of events obtained with an integrated luminosity of 500, 300, 300 pb^{-1} respectively, is also indicated.

Fig.3 Angular distribution of $e^+e^- \rightarrow HZ$ versus $|\cos\vartheta|$ at NLC (1 TeV), for $m_H = 80\text{GeV}$, SM and NP contributions due to \mathcal{O}_{UB} , \mathcal{O}_{UW} , and $\mathcal{O}_{\Phi 2}$. For $f_{\Phi 2} = 0.01$ the curve coincides with the one for $d = -0.01$. The number of events obtained with an integrated luminosity of 80 fb^{-1} is also indicated.

Fig.4 Azimuthal asymmetry A_{14} versus total e^+e^- energy for $m_H = 80\text{GeV}$, SM and NP contributions due to \mathcal{O}_{UW} , (a) $Z \rightarrow b\bar{b}$, (b) $Z \rightarrow \mu^+\mu^-$.

Fig.5 Azimuthal asymmetry A_{12} versus total e^+e^- energy for $m_H = 80\text{GeV}$, SM and NP contributions due to $\overline{\mathcal{O}}_{UW}$, (a) $Z \rightarrow b\bar{b}$, (b) $Z \rightarrow \mu^+\mu^-$.

Fig.6 Azimuthal asymmetry A_{13} versus total e^+e^- energy for $m_H = 80\text{GeV}$, SM and NP contributions due to $\overline{\mathcal{O}}_{UW}$.

Fig.7 Azimuthal asymmetry A_8 versus total e^+e^- energy for $m_H = 80\text{GeV}$, SM and NP contributions due to \mathcal{O}_{UW} .

Fig.8 Angular distribution of $e^+e^- \rightarrow H\gamma$ versus $|\cos\vartheta|$ at the LEP2 energy 192GeV, for $m_H = 80\text{GeV}$ (a), or $m_H = 120\text{GeV}$ (b). The SM and NP contributions are due to \mathcal{O}_{UW} . For \mathcal{O}_{UB} similar results are obtained provided $d_B \sim d/2$. The number of events obtained with an integrated luminosity of 300 pb^{-1} is also indicated.

Fig.9 Angular distribution of $e^+e^- \rightarrow H\gamma$ versus $|\cos\vartheta|$ at NLC (1 TeV), for $m_H = 80\text{GeV}$, (a) SM and NP contributions due to \mathcal{O}_{UW} , (b) SM and NP contributions due to \mathcal{O}_{UB} . The number of events obtained with an integrated luminosity of 80 fb^{-1} is also indicated.

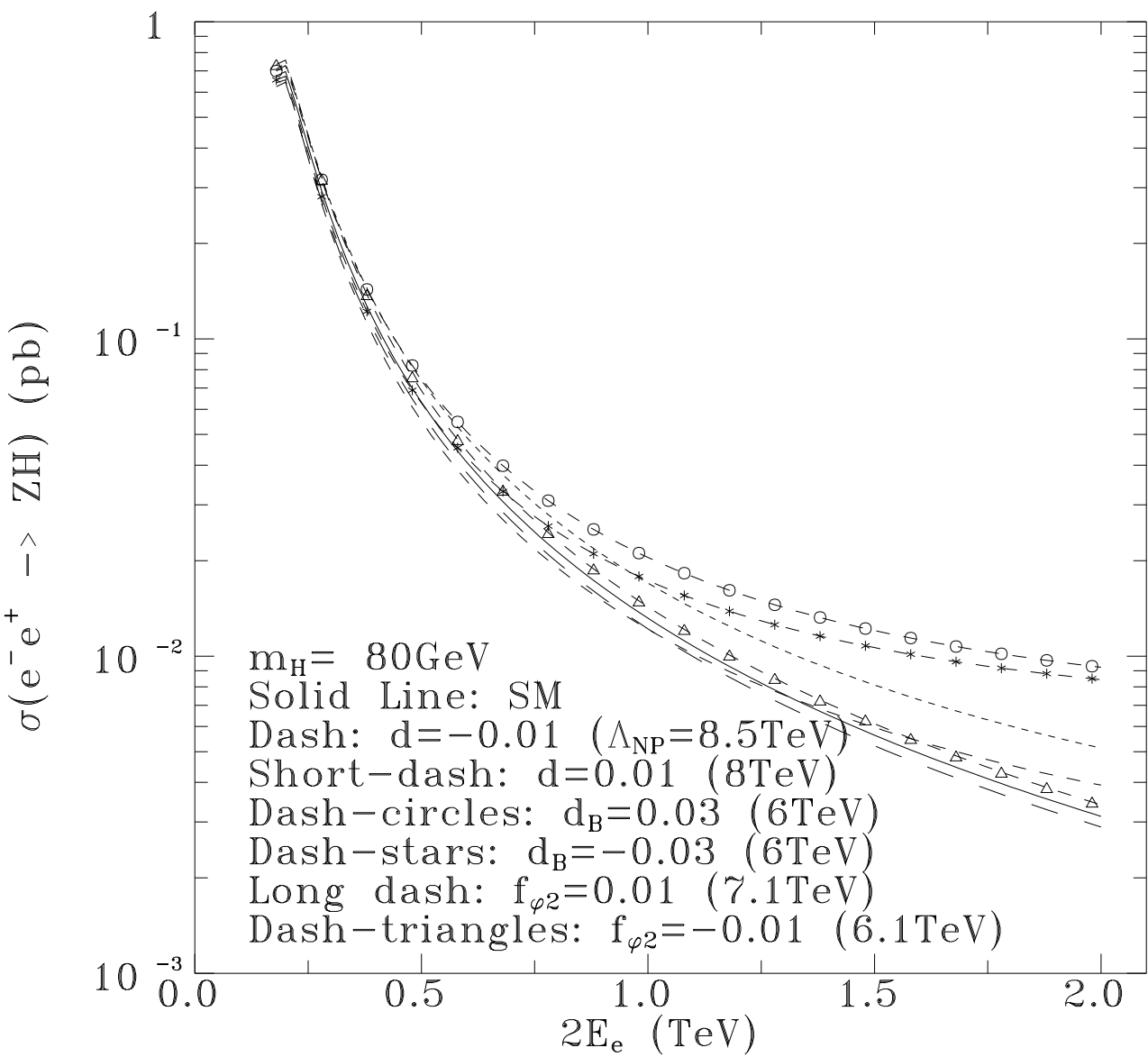


Fig 1

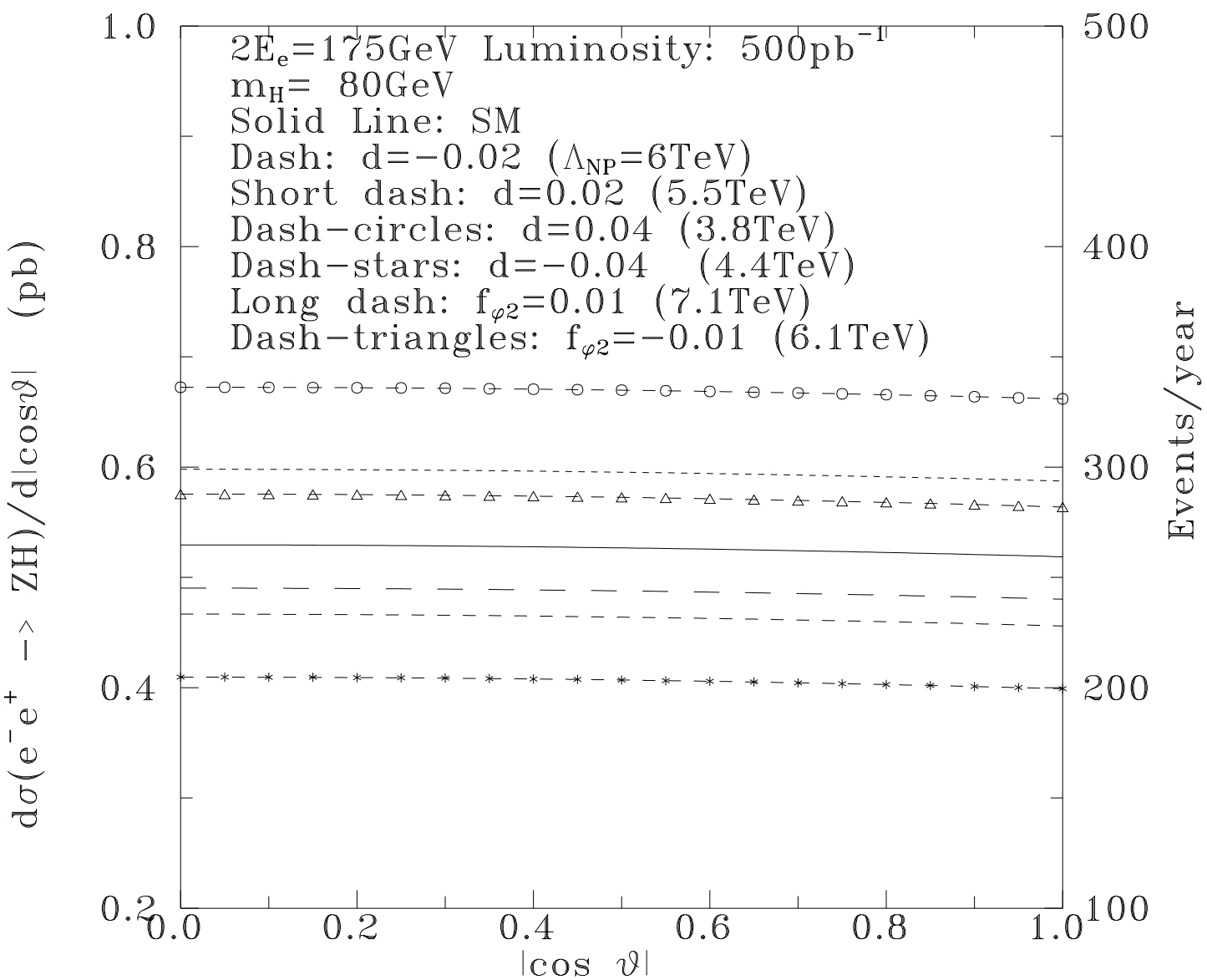


Fig 2a

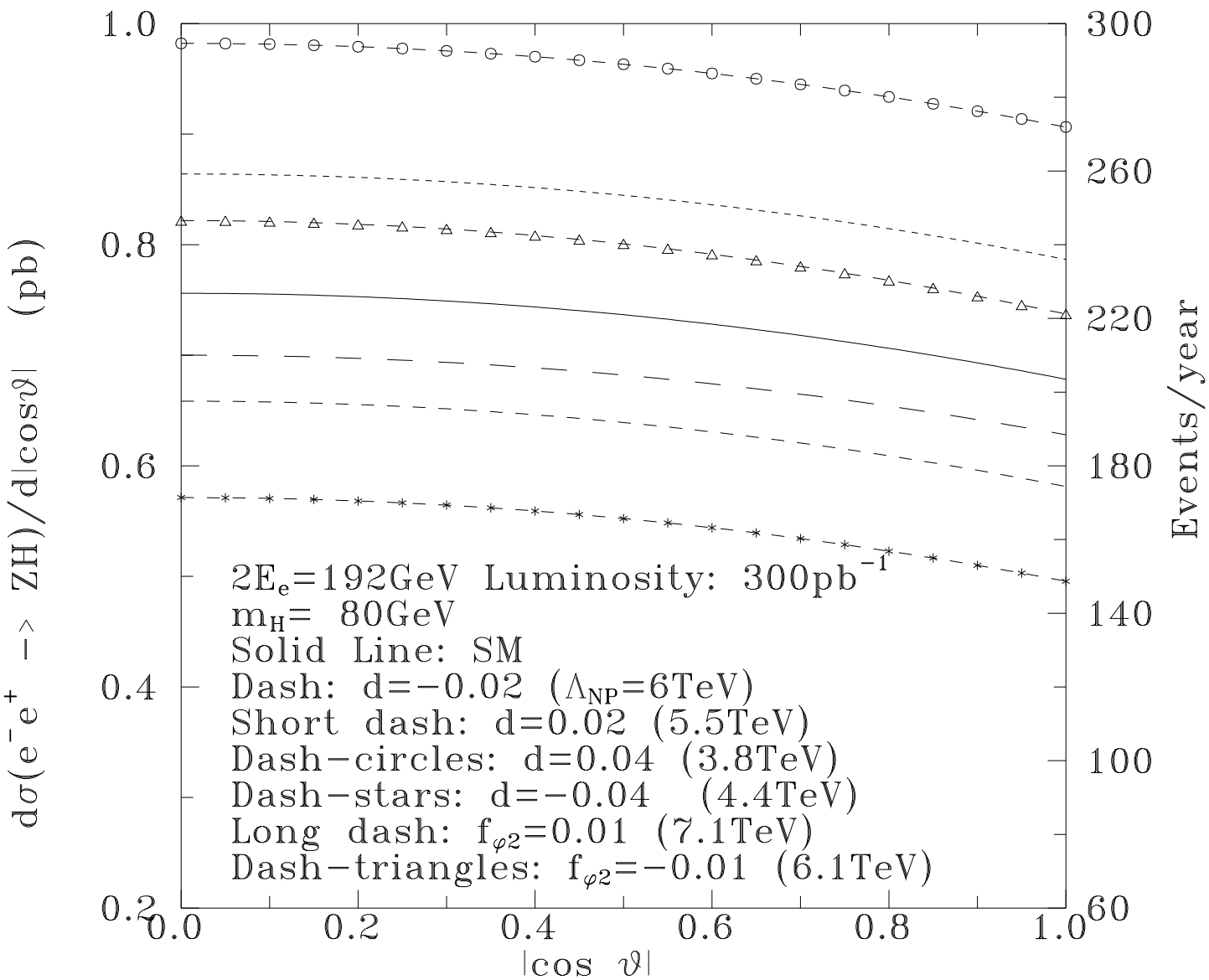


Fig 2b

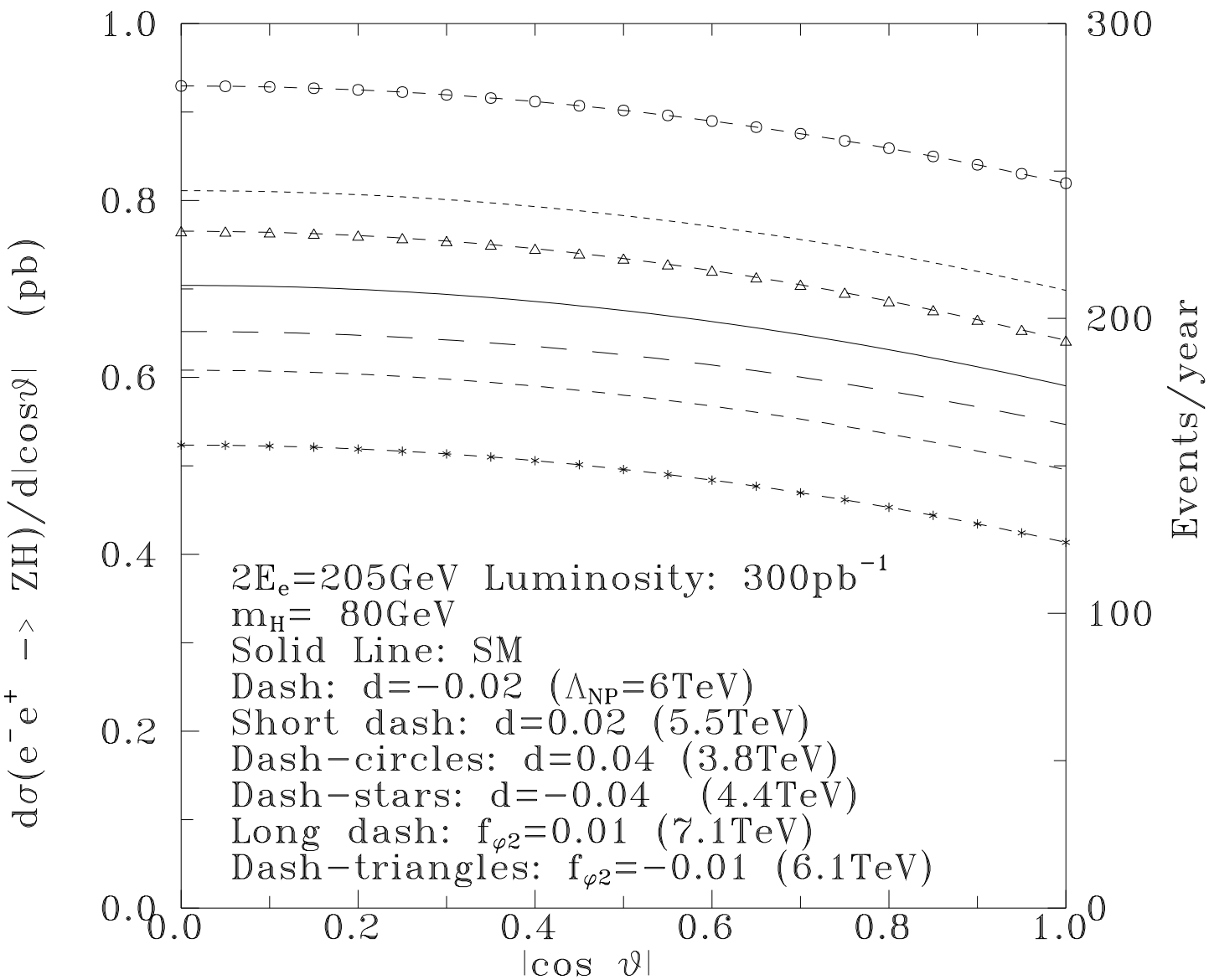


Fig 2c

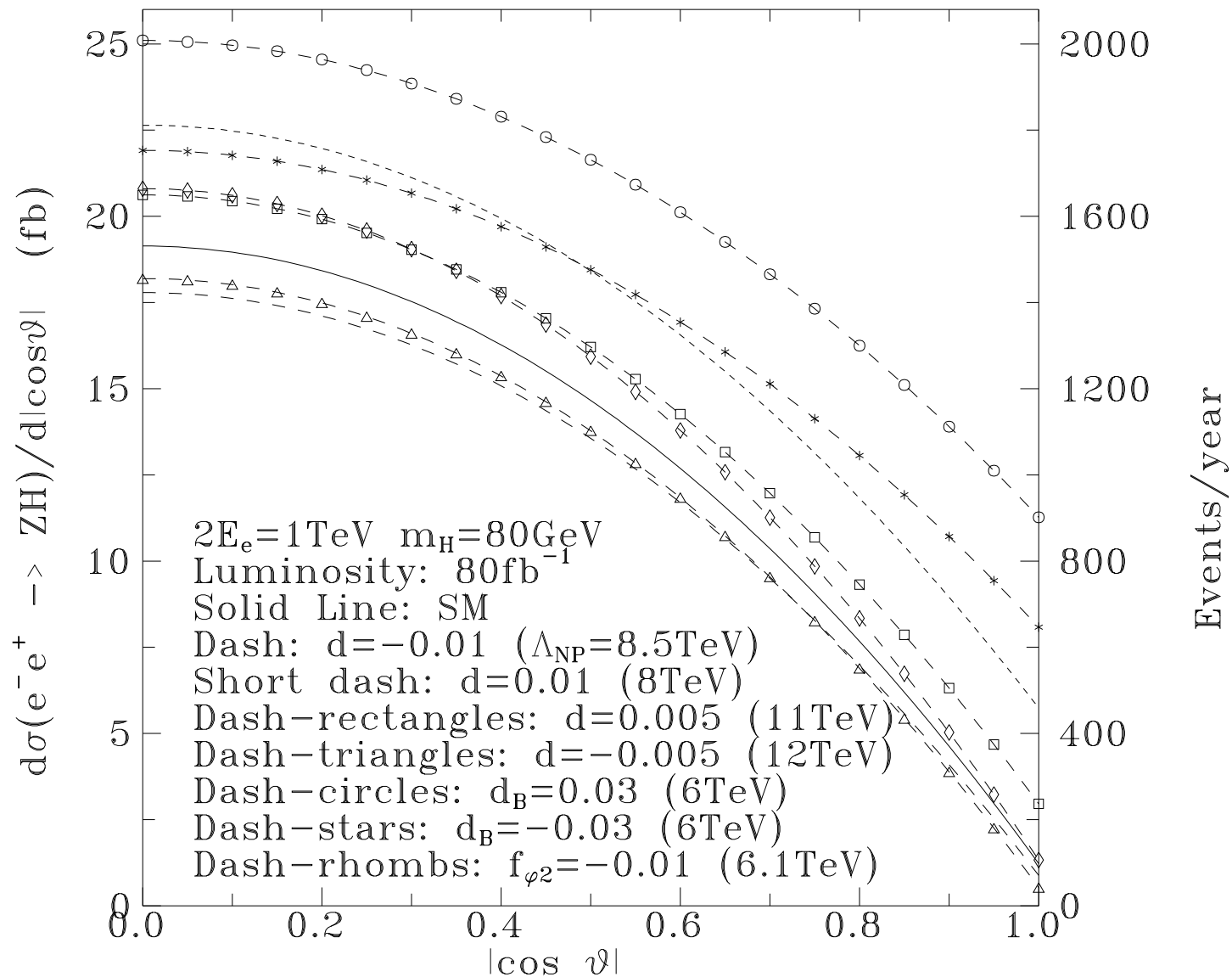


Fig 3

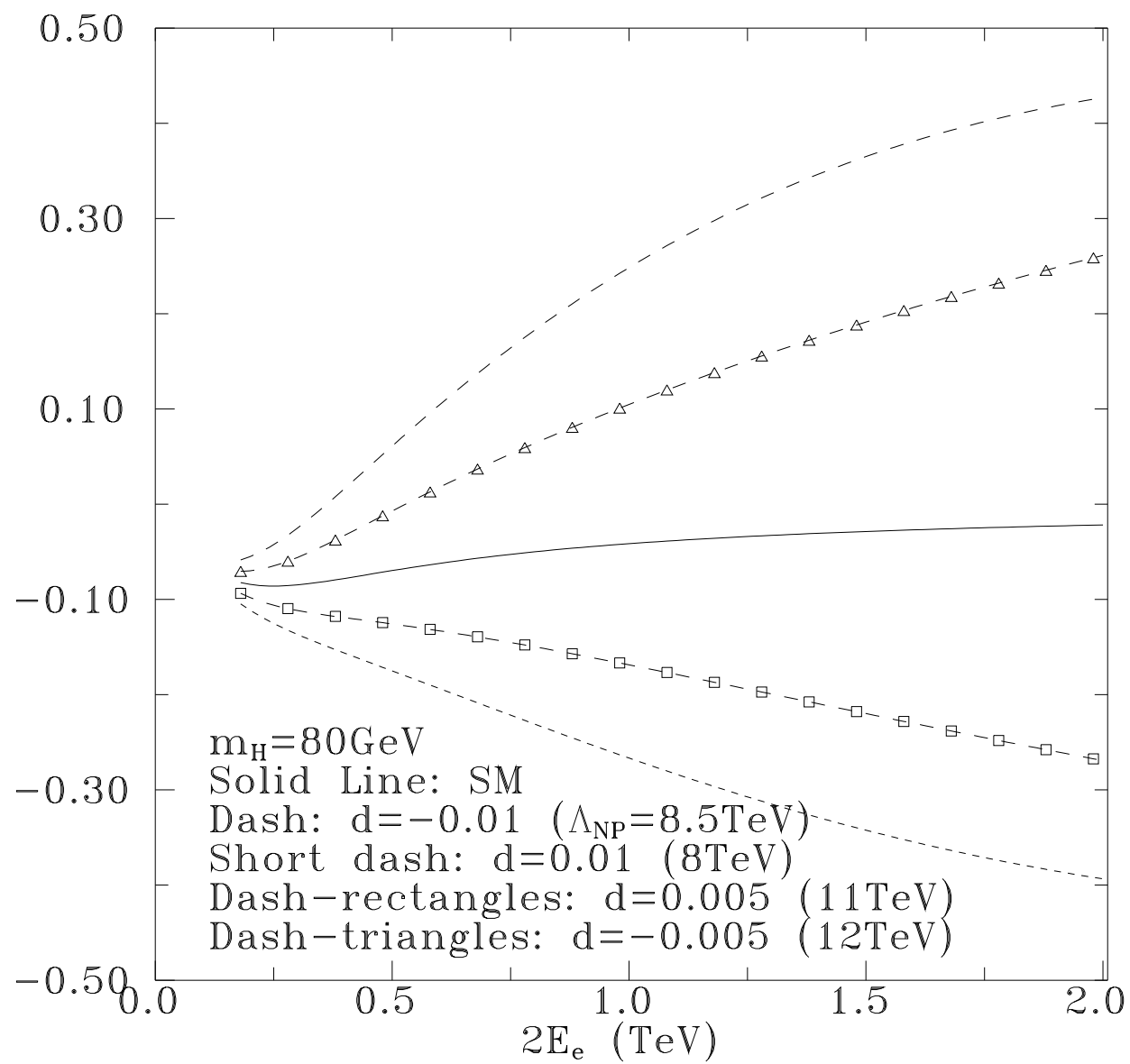


Fig 4a

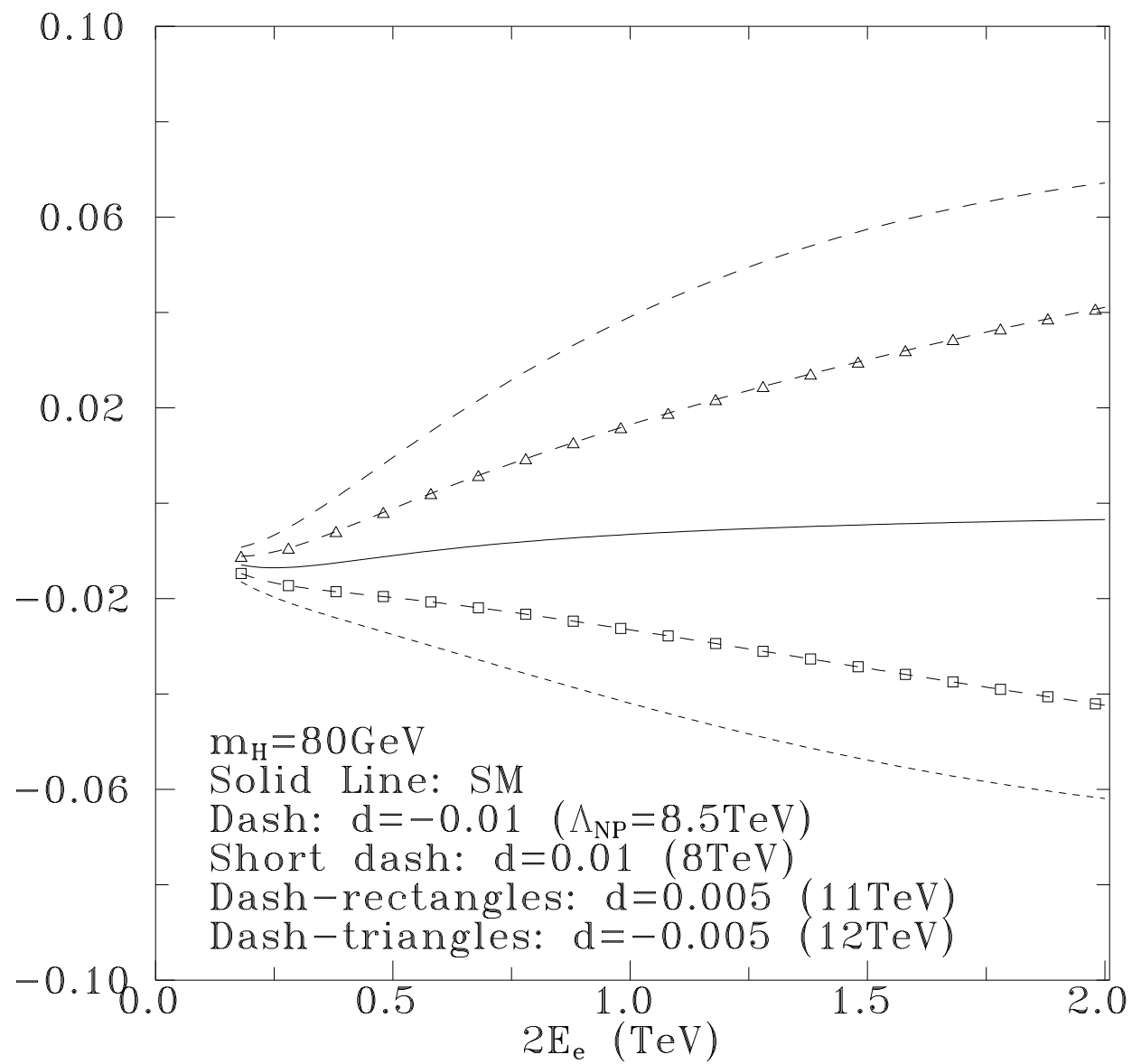


Fig 4b

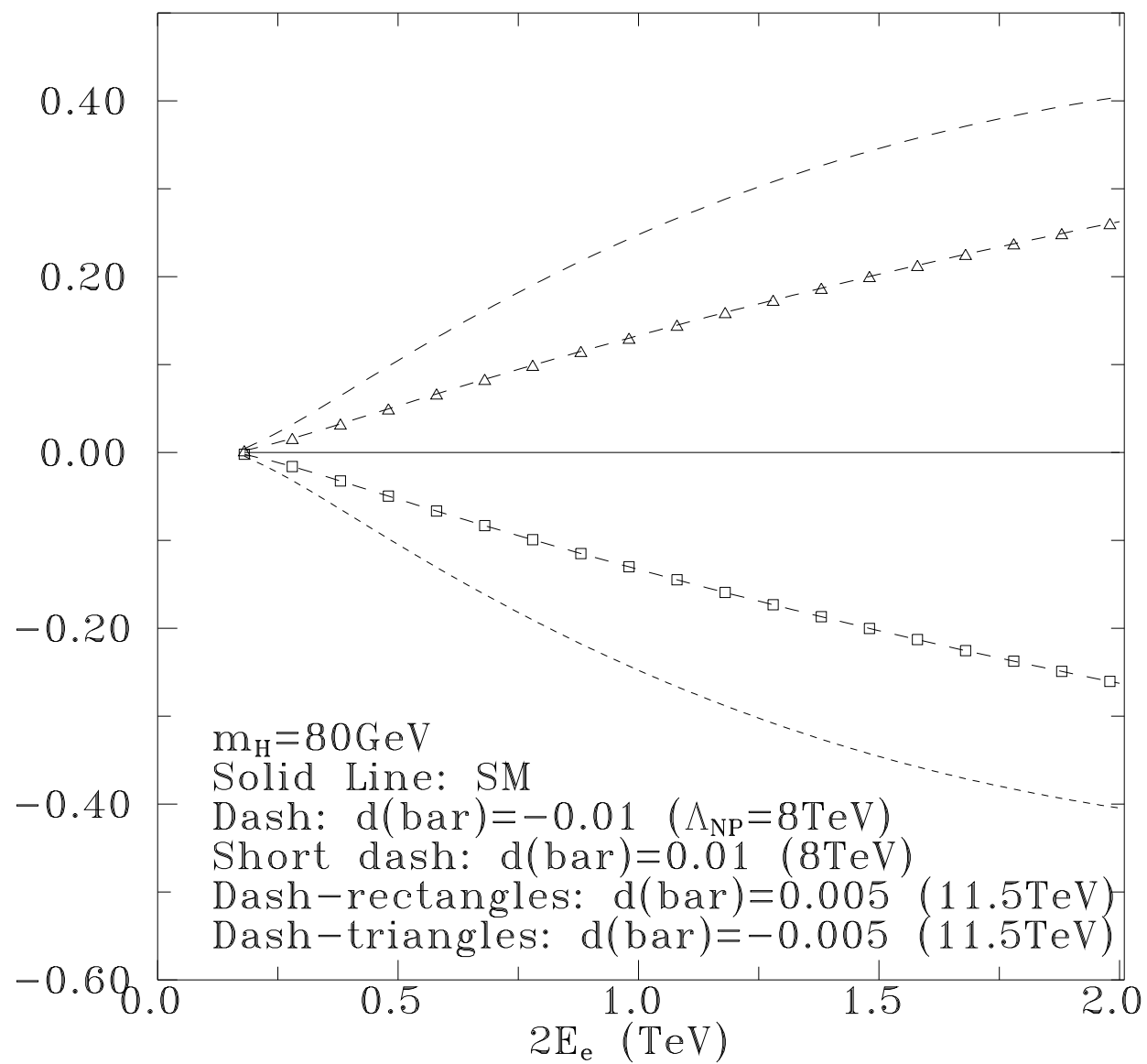


Fig 5a

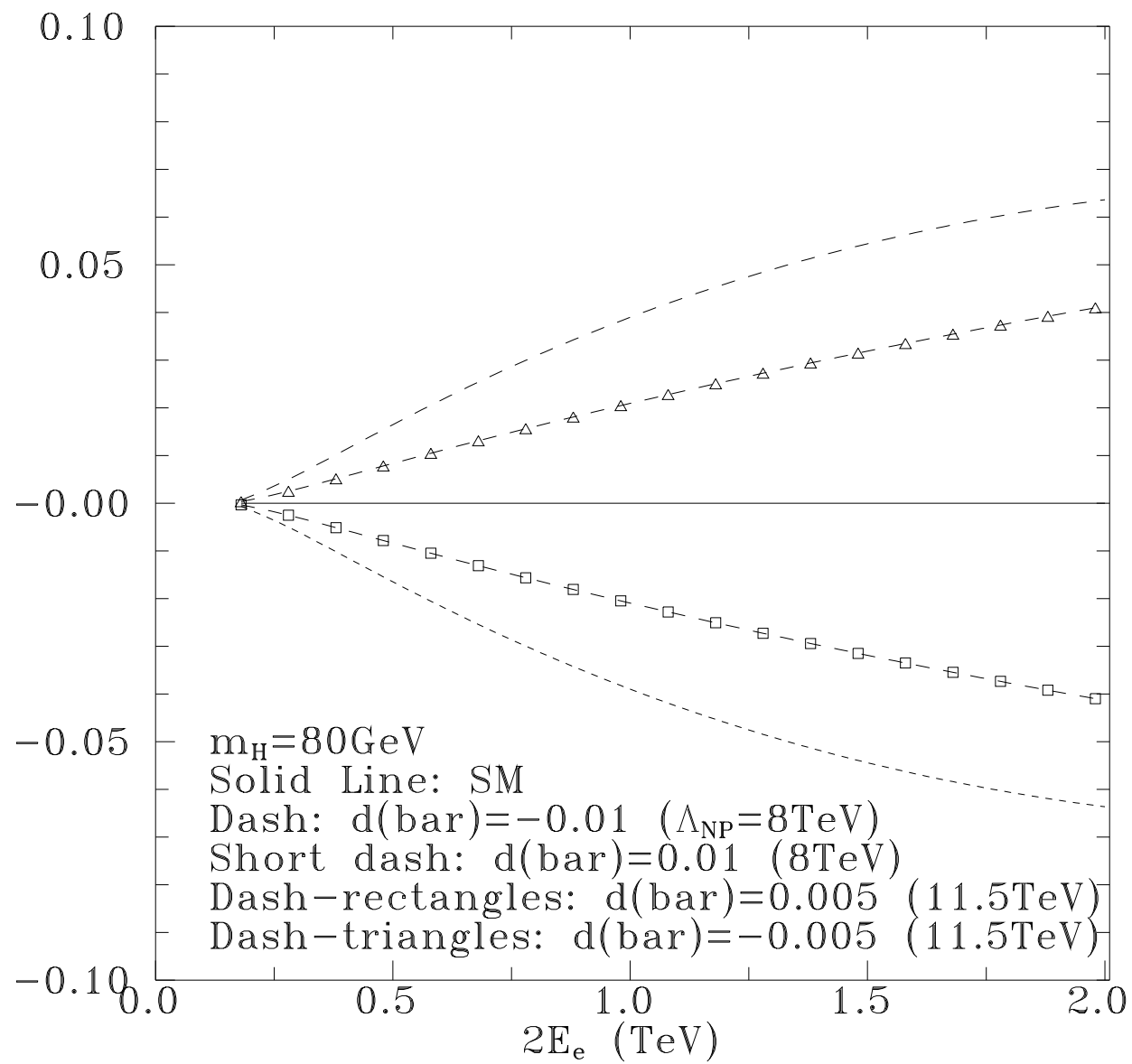


Fig 5b

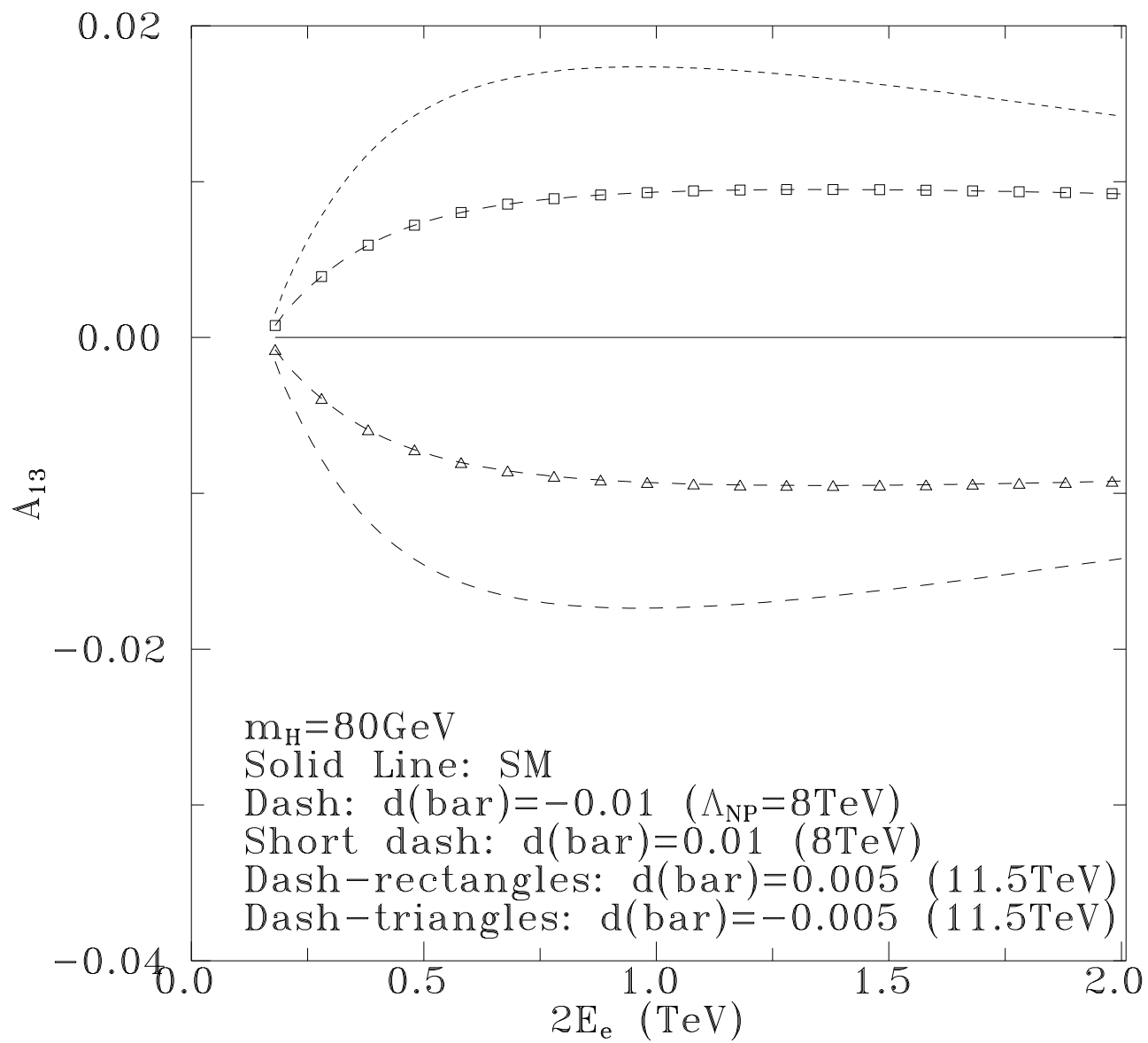


Fig 6

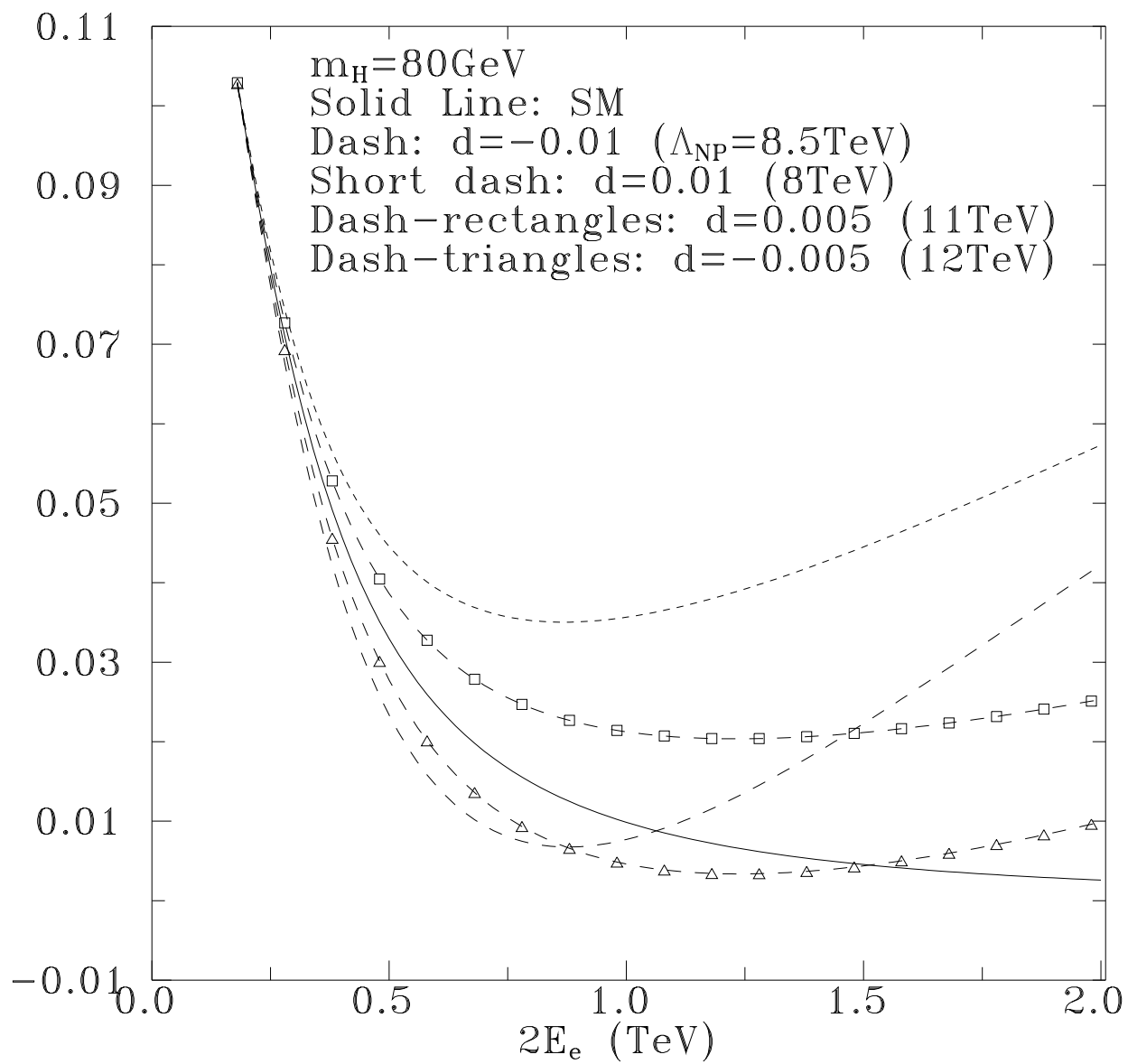


Fig 7

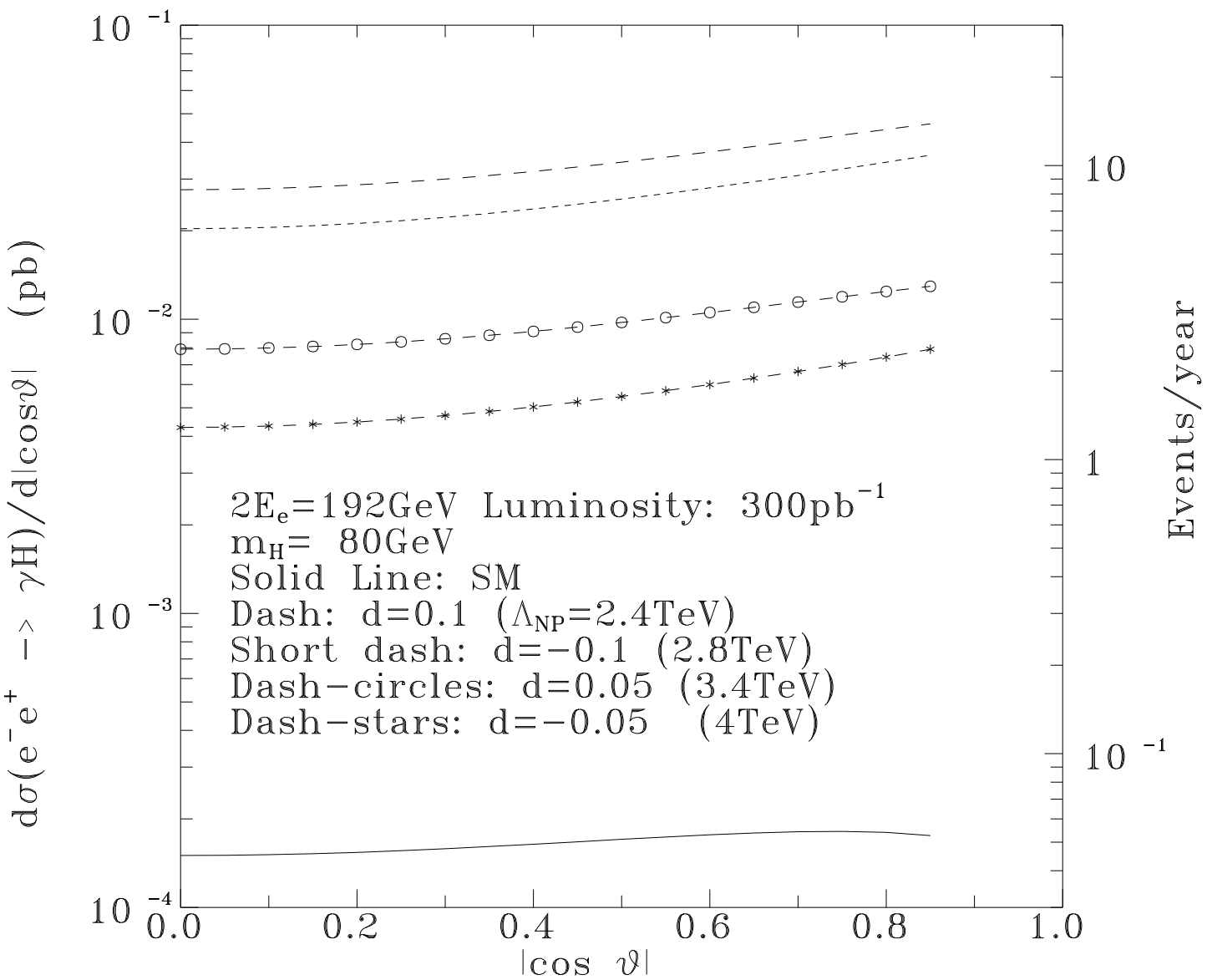


Fig 8a

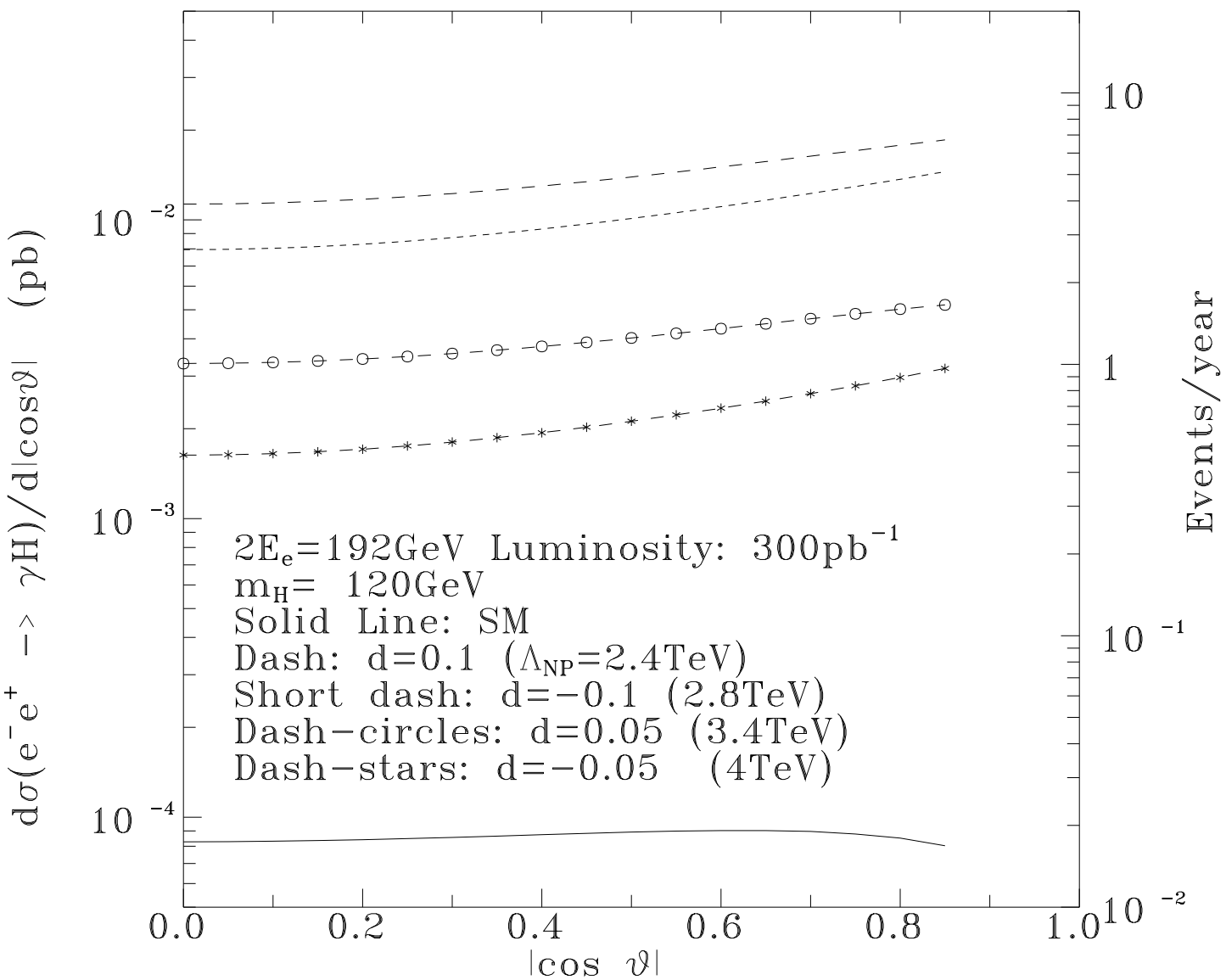


Fig 8b

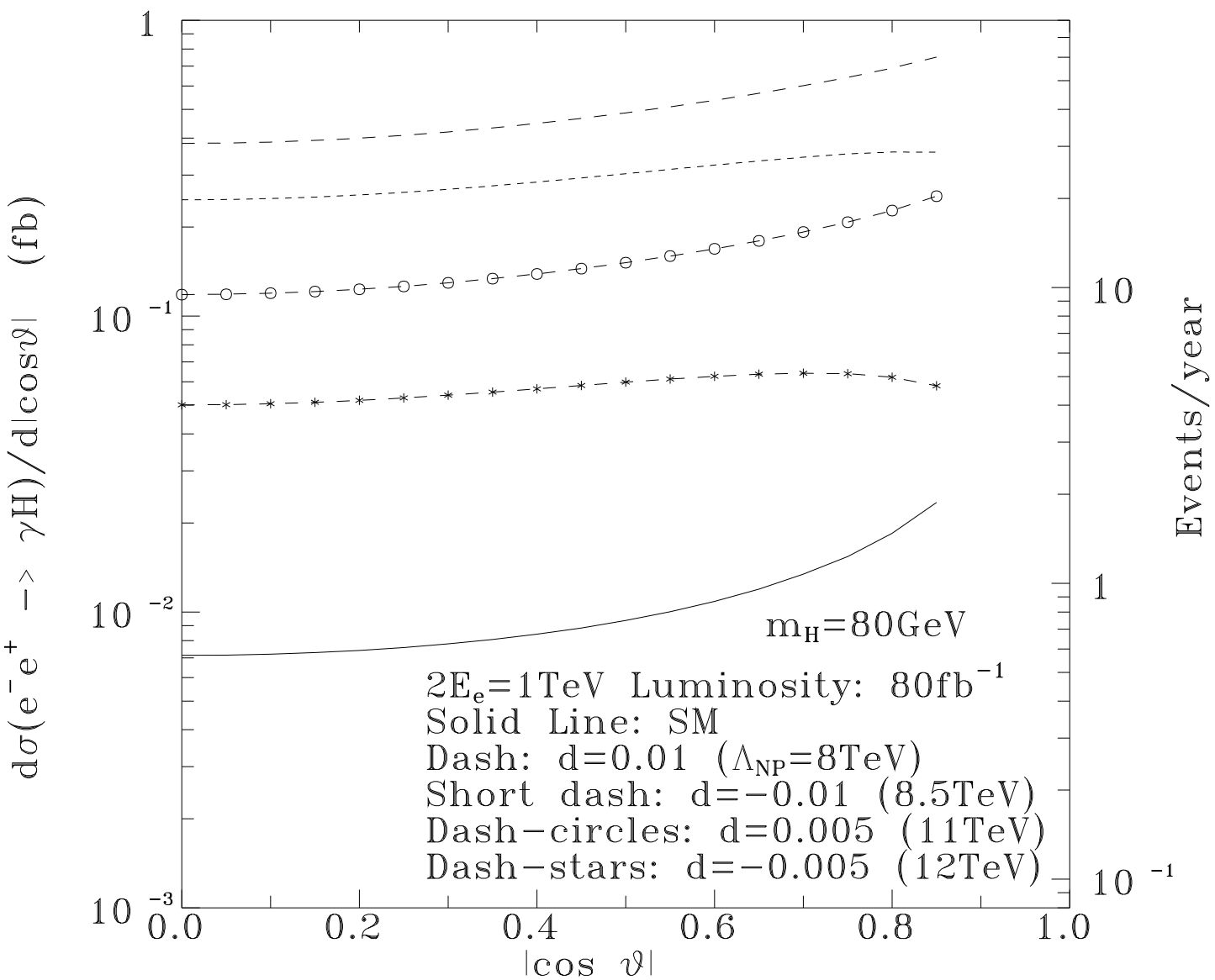


Fig 9a

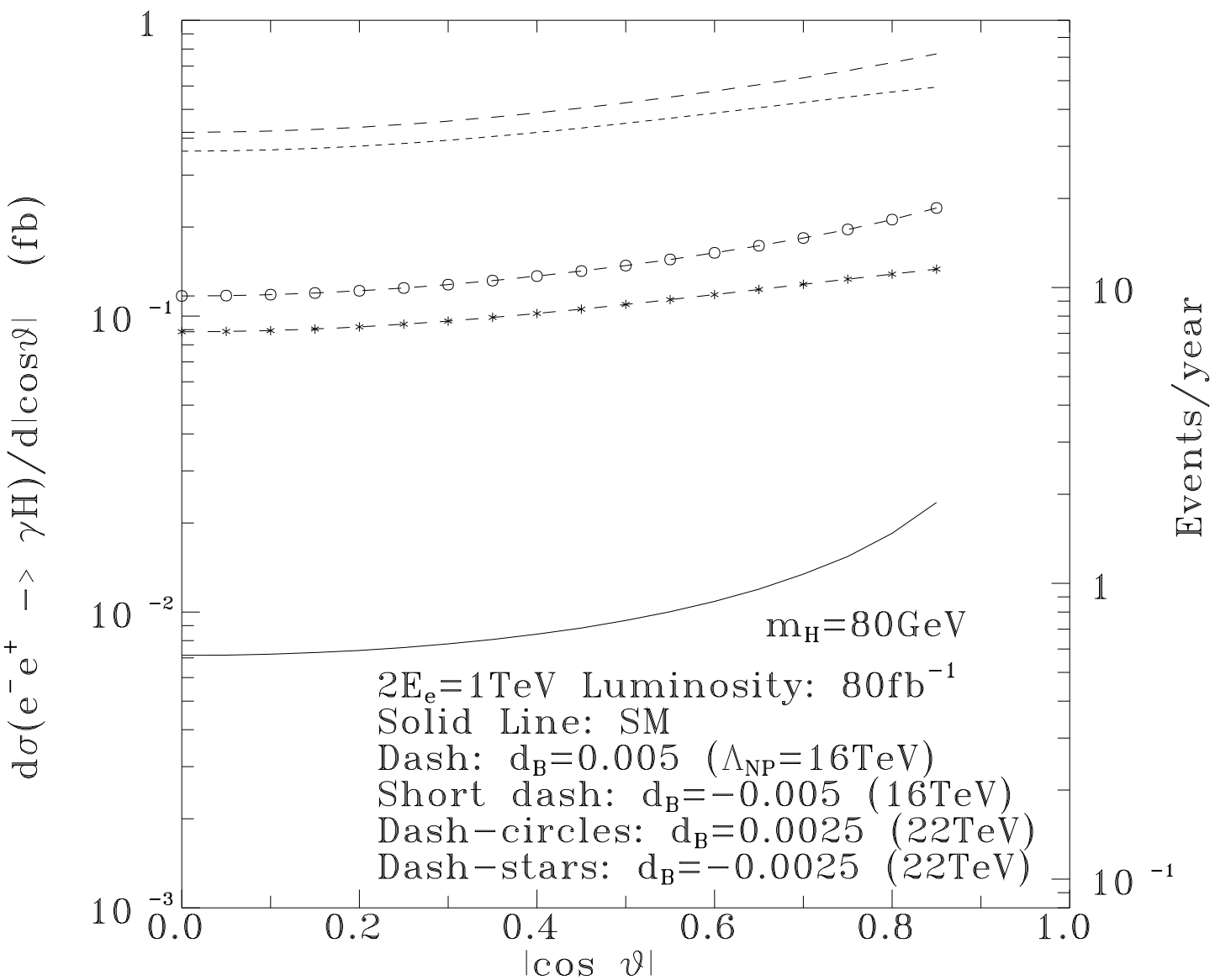


Fig 9b